Physics Letters B 839 (2023) 137776

Contents lists available at ScienceDirect

Physics Letters B

journal homepage: www.elsevier.com/locate/physletb

Neutrino capture on tritium as a probe of flavor vacuum condensate and dark matter

A. Capolupo, A. Quaranta *

Dipartimento di Fisica "E.R. Caianiello" Università di Salerno, and INFN – Gruppo Collegato di Salerno, Via Giovanni Paolo II, 132, 84084 Fisciano (SA), Italy

ARTICLE INFO

Article history:
Received 14 November 2022
Received in revised form 10 January 2023
Accepted 12 February 2023
Available online xxxx
Editor: B. Balantekin

ABSTRACT

We show that the study of neutrino capture on tritium, for non-relativistic neutrinos, can allow to distinguish among the various neutrino models, eventually prove the quantum field theory condensation effects and permit to test the hypothesis according to which the flavor vacuum energy gives a contribution to the dark matter of the universe. Indeed, we show that the capture rate depends on the neutrino model considered, and that it brings an imprint of the flavor vacuum condensate. Experiments like PTOLEMY, designed to reveal the cosmic neutrino background, then can give an indication of the existence of the dark matter component induced by neutrino mixing.

1. Introduction

Neutrino oscillations, which by now have accumulated a significant amount of experimental confirmations [1–4], are a compelling evidence for non-vanishing neutrino masses and for physics beyond the standard model of particles [5–8]. The quantum mechanical theory of neutrino oscillations was originally put forward by Pontecorvo [9,10] and is today widely accepted in its 3-flavor guise. Notwithstanding the consensus on the basic mechanism of neutrino oscillations, neutrino physics is still beset by a number of open issues. The origin of neutrino masses, the fundamental nature (Dirac or Majorana) of neutrinos, the existence of additional flavors, as well as the correct field theoretical description of neutrino mixing, remain debated. On the other hand neutrinos play a major role in cosmology and astrophysics. They figure within leptogenesis scenarios to explain the original baryon asymmetry and sterile neutrinos may contribute to dark matter [11,12].

Originally introduced to explain the rotation curves of galaxies [13], dark matter [14,15] is one of the long-standing puzzles in modern cosmology. Dark matter is modelled as a pressure-less perfect fluid and is believed to account for about 85% of the total matter content of the universe. There is no general consensus on the composition of the mysterious substance. Several explanations for the "missing matter" have been proposed, including primordial black holes [16,17], supersymmetric particles [18], axions [19–21] and sterile neutrinos [12,22].

In recent years a new connection between neutrino mixing and cosmology has emerged. One of the possible quantum field theory (QFT) models of neutrino mixing, based on the flavor Hilbert space [23–25], involves a condensed vacuum state, the "flavor vacuum". Due to its condensate structure the flavor vacuum yields a purely quantum field theoretical contribution to the energy-momentum tensor of matter. Remarkably, the energy-momentum tensor associated to the flavor vacuum is that of a pressure-less perfect fluid [28–32]. Consequently the flavor vacuum may possibly represent a dark matter component.

Testing this hypothesis proves to be a formidable task for the present possibilities. The same mechanism underlying the flavor vacuum condensation is responsible for QFT modifications to the neutrino oscillation formulas. Yet these modifications are mostly negligible except for non-relativistic neutrinos $E_\nu \simeq m_\nu$, whereas neutrino oscillations are usually accessible at much larger neutrino energies $E_\nu \gg m_\nu$. This rules out oscillation experiments as a possible probe of the condensation mechanism. There are, however, experiments aimed at the revelation of non-relativistic neutrinos, like PTOLEMY [33], where the QFT effects may be observable.

In recent years several investigations have been devoted to the capture of the cosmic neutrino background, both in the context of the PTOLEMY experiment [34] and of the KATRIN experiment [35]. In this article we show that also other aspects of neutrino physics may be accessible via low energy experiments. We discuss the possibility of testing the QFT of neutrino mixing and the related dark-matter-like

* Corresponding author.
E-mail addresses: capolupo@sa.infn.it (A. Capolupo), anquaranta@unisa.it (A. Quaranta).

https://doi.org/10.1016/j.physletb.2023.137776

contribution by means of low energy neutrino experiments such as PTOLEMY. We study the QFT condensation effect on the basic detection process, the neutrino capture on tritium. We show that the capture rate depends on the neutrino model considered, and, in particular, that it bears a trace of the flavor vacuum condensate. We argue that low energy neutrino experiments may not only distinguish among the possible QFT formulations of neutrino mixing, but also indirectly probe the hypothesis of the flavor vacuum as a dark matter component.

The paper is structured as follows. In section 2 we elucidate the connection between neutrino mixing and dark matter, recalling the main results in this respect. In section 3 we present the basic amplitude for the inverse beta decay and discuss the four possible choices of neutrino states according to the known neutrino mixing schemes. In section 4 we compute the capture cross sections and the capture rates corresponding to each of the four choices of neutrino states, showing the observable effects due to the flavor vacuum condensation. The last section is devoted to the conclusions.

2. Cosmological effects from the QFT of neutrino mixing

The quantum mechanical theory of neutrino oscillations pioneered by Pontecorvo [9,10] is sufficient to explain most of the observed phenomenology regarding neutrinos. The corresponding quantum field theory, however, is still lacking a universally accepted formulation. In particular, it is debated whether the basic quantum fields are the massive fields ν_1, ν_2, ν_3 which propagate freely in vacuum, or the flavor fields ν_e, ν_μ, ν_τ, which are those appearing in the weak interaction vertices. In the "flavor Fock space" approach [23–25] flavor fields are the fundamental entities and the usual mixing relations between neutrino states are elevated to relations between the quantum fields:

$$\nu_e(x) = \cos\Theta\ \nu_1(x) + \sin\Theta\ \nu_2(x)\ ; \qquad \nu_\mu(x) = \cos\Theta\ \nu_2(x) - \sin\Theta\ \nu_1(x)\ , \tag{1}$$

where we have considered two flavors with mixing angle Θ for definiteness. This corresponds to neutrinos which are produced and detected as flavor states. Such an approach is substantiated by the observation that in the weak interaction vertices neutrinos appear as states with a definitive flavor, so to ensure lepton number conservation in the vertices. Because mixing is here stated at the level of fields, the corresponding 1-particle states $|\nu_\sigma\rangle$ (see note [49]) are mixed everywhere on spacetime, that is, regardless of the particular spacetime position x. This means that the 1-particle states defined by the flavor operators are always given by linear combinations of mass states. In particular, if the mass states are taken as plane waves, no kinematic decoherence occurs, otherwise, considering, e.g. wave packets, one can have kinematic decoherence. We here employ plane wave states and disregard the effect of kinematic decoherence on the mass states. We point out a fundamental aspect of the quantum field theory of neutrino mixing which is absent in the quantum mechanical treatment. In quantum mechanics, given the finite number of degrees of freedom, it holds the Stone-Von Neumann theorem, which ensures the equivalence of all the representations and of all the Hilbert spaces. In quantum field theory, where the degrees of freedom are infinite, the theorem ceases to hold and there are infinitely many inequivalent representations, corresponding to distinct and mutually orthogonal Fock spaces [26]. The choice of the appropriate Fock space for the particle interpretation of the theory must hence be dictated by physical arguments. In the case of neutrino mixing, in particular, the Fock spaces corresponding to the mass and the flavor representations are unitarily inequivalent [27]. Therefore the choice of different Hilbert spaces can lead to different physical results and care is required in the choice of the appropriate representation. In the flavor Fock space approach the choice is the flavor representation, because in the production and detection vertices neutrinos appear as flavor states. In this approach, Eq. (1) is recast in terms of a mixing generator $G_\Theta(t)$ as [23–25]

$$\nu_e(x) = G_\Theta^{-1}(t)\nu_1(x)G_\Theta(t)\ ; \quad \nu_\mu(x) = G_\Theta^{-1}(t)\nu_2(x)G_\Theta(t)$$

whose form is found to be $G_\Theta(t) = \exp[\Theta((\nu_2, \nu_1)_t - (\nu_1, \nu_2)_t)]$, with $(,)_t$ denoting the Dirac inner product on the hypersurface $x^0 = t$. The action of the generator is then taken to *define* the flavor annihilators as

$$a^s_{\boldsymbol{k},\nu_e}(t) = G_\Theta^{-1}(t)a^s_{\boldsymbol{k},1}G_\Theta(t) = \cos\Theta\ a^s_{\boldsymbol{k},1} + \sin\Theta\left(U^*_{\boldsymbol{k}}(t)a^s_{\boldsymbol{k},2} + \epsilon^s V_{\boldsymbol{k}}(t)b^{s\dagger}_{-\boldsymbol{k},2}\right)$$

and similar for $a^s_{\boldsymbol{k},\nu_\mu}, b^s_{\boldsymbol{k},\nu_e}, b^s_{\boldsymbol{k},\nu_\mu}$, with $s = \pm 1/2$ and $\epsilon^s = (-1)^{s-\frac{1}{2}}$. The flavor operators are then expressed in terms of the mass operators through a Bogoliubov transformation nested into a rotation. The terminology is justified by noting that the coefficients $U_{\boldsymbol{k}}(t) = (u_{\boldsymbol{k},2}, u_{\boldsymbol{k},1})_t$, $V_{\boldsymbol{k}}(t) = (u_{\boldsymbol{k},1}, v_{\boldsymbol{k},2})_t$, given by the scalar products of modes with positive u and negative energy v, satisfy the identity $|U_{\boldsymbol{k}}(t)|^2 + |V_{\boldsymbol{k}}(t)|^2 = 1$. For completeness we give the explicit expressions for the Bogoliubov coefficients:

$$\begin{aligned} &U_{\boldsymbol{k}}(t) = |U_{\boldsymbol{k}}|e^{i(\omega_{\boldsymbol{k},2}-\omega_{\boldsymbol{k},1})t} \quad ; \qquad V_{\boldsymbol{k}}(t) = |V_{\boldsymbol{k}}|e^{i(\omega_{\boldsymbol{k},2}+\omega_{\boldsymbol{k},1})t} \\ &|U_{\boldsymbol{k}}| = \sqrt{\frac{\omega_{\boldsymbol{k},2}+m_1}{2\omega_{\boldsymbol{k},1}}}\sqrt{\frac{\omega_{\boldsymbol{k},2}+m_2}{2\omega_{\boldsymbol{k},2}}}\left(1 + \frac{\boldsymbol{k}^2}{(\omega_{\boldsymbol{k},1}+m_1)(\omega_{\boldsymbol{k},2}+m_2)}\right) \\ &|V_{\boldsymbol{k}}| = \sqrt{\frac{\omega_{\boldsymbol{k},2}+m_1}{2\omega_{\boldsymbol{k},1}}}\sqrt{\frac{\omega_{\boldsymbol{k},2}+m_2}{2\omega_{\boldsymbol{k},2}}}\left(\frac{|\boldsymbol{k}|}{(\omega_{\boldsymbol{k},2}+m_2)} - \frac{|\boldsymbol{k}|}{(\omega_{\boldsymbol{k},1}+m_1)}\right)\ , \end{aligned} \tag{2}$$

with $\omega_{\boldsymbol{k},j} = \sqrt{\boldsymbol{k}^2 + m_j^2}$ for $j = 1, 2$. The appearance of a mass creation operator in the expression of the flavor annihilators signals that the representation defined by the flavor operators is unitarily inequivalent to the representation defined by the mass annihilators. In particular, the flavor annihilators define a time-dependent vacuum state, the flavor vacuum $|0_F(t)\rangle$, which is distinct from the mass vacuum $|0_M\rangle$.[1]

[1] Notice that the 1-particle states for mixed neutrinos are obtained by applying the flavor creation operators on the flavor vacuum

$$a^{s\dagger}_{\boldsymbol{k},\nu_\sigma}(t)\,|0_F(t)\rangle = |\nu_{\sigma,\boldsymbol{k},s}(t)\rangle \tag{3}$$

for $\sigma = e, \mu$.

Here the vacuum states are explicitly given by $|0_M\rangle = |0_1\rangle \otimes |0_2\rangle$ and $|0_F(t)\rangle = |0_e(t)\rangle \otimes |0_\mu(t)\rangle$, where the states $|0_1\rangle$, $|0_2\rangle$ are annihilated by the operators a_1, a_2 and the states $|0_e(t)\rangle$, $|0_\mu(t)\rangle$ are annihilated by the operators $a_{\nu_e}(t), a_{\nu_\mu}(t)$.

Remarkably, the flavor vacuum has the structure of a condensate of particle-antiparticle pairs with definite masses [23–25]. An important remark is that the flavor vacuum contains both left-handed and right-handed neutrinos and antineutrinos, in the Dirac case, while it only contains left-handed neutrinos and right-handed antineutrinos in the Majorana case. Here we will mainly focus on the Dirac flavor vacuum. The condensate structure is apparent if one computes the number expectation values on the flavor vacuum

$$N^F_{\boldsymbol{k},i} = \langle 0_F(t)| a^\dagger_{\boldsymbol{k},i} a_{\boldsymbol{k},i} |0_F(t)\rangle = \sin^2\Theta |V_{\boldsymbol{k}}|^2 = \langle 0_F(t)| b^\dagger_{\boldsymbol{k},i} b_{\boldsymbol{k},i} |0_F(t)\rangle \ , \tag{4}$$

which holds for any $i = 1, 2$ and any $\boldsymbol{k}$. The quantity $\sin^2\Theta|V_{\boldsymbol{k}}|^2$ plays the role of a condensation density. Notice that $N^F_{\boldsymbol{k},i}$ can be equivalently expressed as $N^F_{\boldsymbol{k},i} = \langle 0_M| a^\dagger_{\boldsymbol{k},\sigma} a_{\boldsymbol{k},\sigma} |0_M\rangle$, with $\sigma = e, \mu$. This simply follows from equation (4) by inserting the identity $1 = G_\Theta(t) G^{-1}_\Theta(t)$ on the left and on the right of the number operator $a^\dagger_{\boldsymbol{k},i} a_{\boldsymbol{k},i}$.

It can be shown that, as a consequence of the condensate structure, a non-vanishing energy momentum tensor $T_{\mu\nu}$ is associated to the flavor vacuum. Specifically, the pressure p is found to vanish, due to a vanishing expectation value of the spatial components of the energy momentum tensor $\langle 0_F(t)| T^i_i |0_F(t)\rangle = 0$. On the other hand, the flavor vacuum is associated with a non zero energy density given by [29–32]

$$\rho = \langle 0_F(t)| T^0_0 |0_F(t)\rangle = 8\sin^2\Theta \int d^3k \left(\omega_{\boldsymbol{k},1} + \omega_{\boldsymbol{k},1}\right) |V_{\boldsymbol{k}}|^2 \ . \tag{5}$$

Here $\omega_{\boldsymbol{k},j} = \sqrt{\boldsymbol{k}^2 + m_j^2}$ for $j = 1, 2$. As it is evident from equation (5), the energy density vanishes in absence of mixing $\Theta = 0$ and for $V_{\boldsymbol{k}} = 0$. Therefore it is a direct consequence of the unitarily inequivalence between the flavor and the mass representations. Not only is the flavor vacuum associated with a non vanishing energy momentum tensor, but its components satisfy the equation of state [29–32]

$$p = w\rho = 0 \ \longrightarrow \ w = 0 \ \ (\rho \neq 0) \ , \tag{6}$$

which is typical of dust and cold dark matter [13–15]. The results (5) and (6) were derived in flat space, but already provide an indication of the possibility that the flavor vacuum may contribute to cold dark matter, due to its condensate structure.

A stronger hint to such a possibility comes from the curved spacetime generalization of the flavor Fock space approach [28,36]. Much of the formalism, including the condensate structure of the flavor vacuum, is common to the flat space theory. The main advantage is that in curved spacetime the energy momentum tensor associated to the flavor vacuum can be consistently studied within the semiclassical approach, where it appears on the right hand side of the Einstein field equations as a proper source term. Even if the analysis, in this respect, is still ongoing and must be extended to other metrics, recent results show that also in curved space the flavor vacuum satisfies the equation of state of cold dark matter.

For a spatially flat Friedmann-Robertson-Walker metric with De Sitter evolution, at late times, the energy density takes the form [28]

$$\begin{aligned}\rho(\tau) \simeq\ & i\sin^2\Theta \sum_\lambda \int d^3p |\Xi_p(\tau_0)|^2 \left(i\frac{H_0^3\tau^3}{2\pi^3}\right) \sum_{j=1,2} m_j \tanh\left(\frac{\pi m_j}{H_0}\right) \\ & + \frac{i}{2}\sin^2\Theta \sum_\lambda \int d^3p \left[\Xi^*_p(\tau_0)\Lambda_p(\tau_0)\left(\frac{-im_1 H_0^3\tau^3}{2\pi^3\cosh\left(\frac{\pi m_1}{H_0}\right)}\right) - c.c.\right] \\ & - \frac{i}{2}\sin^2\Theta \sum_\lambda \int d^3p \left[\Xi^*_p(\tau_0)\Lambda^*_p(\tau_0)\left(\frac{-im_2 H_0^3\tau^3}{2\pi^3\cosh\left(\frac{\pi m_2}{H_0}\right)}\right) - c.c.\right] \ ,\end{aligned} \tag{7}$$

where τ is the conformal time, H_0 is the constant Hubble factor and Λ, Ξ are the curved space counterparts of U, V (Bogoliubov coefficients). For the details, we refer the reader to the work [28]. The essential point of Eq. (7) is the dependence of the energy density on the mixing angle and on the Bogoliubov coefficients. Just as in flat space, $\rho = 0$ whenever $\Theta = 0$, or $\Xi = 0$. In addition, the pressure p is found to vanish, so that, also in this case, the flavor vacuum satisfies the equation of state (6), typical of cold dark matter. Ongoing studies are aimed at proving the same relation in other classes of metrics.

The results obtained both in flat and in curved spacetime show that the condensate associated to the flavor vacuum might play a role as a cold dark matter component. Given the cosmological and astrophysical relevance of such a possibility, an experimental test of the underlying theory is desirable. Besides the energy-momentum considerations related to the flavor vacuum, the flavor Fock space approach predicts modified oscillation formulas, both in flat and in curved space. These modifications are hard to observe directly, because their magnitude is negligible at almost all the energy scales, except when the neutrino energy is close to the neutrino masses $E \sim m_j$. On the other hand observed neutrinos are all extremely relativistic $E \gg m_j$, so that a direct test of the theory through oscillation experiments is unviable, at least for the current possibilities. A direct test of the cosmological implications is likewise hard to attain due to the large scales involved. For these reasons previous attempts at probing the flavor Fock space model have focused on analogous systems. In [37] it was proposed that Rydberg atoms be used to simulate neutrino mixing and reproduce the resulting condensate, which would leave a signature on the thermodynamic quantities of the system. Recently the impact of the flavor condensate on the beta decay spectrum has also been explored [38].

In this paper we propose that the neutrino capture on tritium be used to probe the flavor Fock space model. Due to the sensitivity of the process to extremely low energy neutrinos, there is a hope that the quantum field theoretic corrections, mostly relevant for non-relativistic ($E \sim m_j$) neutrinos may show up in capture experiments. The quantum field theoretical corrections and the condensation density of Eq. (4) do indeed depend on the Bogoliubov coefficient $V_{\boldsymbol{k}}$. As it can be checked from the definition Eq. (2), $V_{\boldsymbol{k}}$ is negligible at high momenta, where $V_{\boldsymbol{k}} \to 0$ and $U_{\boldsymbol{k}} \to 1$, while it is significantly different from zero for energies close to the neutrino masses $E \sim m_j$. An experiment of this kind is PTOLEMY [33] which is aimed at revealing the extremely non-relativistic neutrinos of the cosmic neutrino background (CνB). In the next sections we show that, if the flavor Fock space approach is valid, the quantum field theoretic corrections show up in the capture rate for neutrinos, which assumes different values according to the neutrino model considered. Experiments aimed at the revelation of the CνB can therefore distinguish among the various neutrino models and eventually validate the hypothesis of the flavor vacuum as a dark matter component.

3. Hamiltonian and neutrino states

We shall be primarily interested in non-relativistic (low energy) neutrinos which constitute the CνB [39,40] and may be probed by the PTOLEMY experiment [33]. The basic reaction for neutrino capture is the inverse beta decay $\nu + n \to e^- + p$. Due to the low neutrino energies involved, the reaction can be safely described with the current-current interaction Hamiltonian [34]:

$$H_I = \frac{G_F}{\sqrt{2}} V_{ud} \left[\bar{p}(x)\gamma_\mu \left(f(0) - g(0)\gamma^5\right) n(x)\right]\left[\bar{e}(x)\gamma^\mu \left(1-\gamma^5\right)\nu_e(x)\right] + h.c.\,. \tag{8}$$

Here $G_F = 1.166 \times 10^{-5}$ GeV^{-2} is the Fermi constant, V_{ud} is the CKM matrix element, $f(q)$ and $g(q)$ are nuclear form factors [41] and $n(x), p(x), e(x), \nu_e(x)$ are respectively the neutron, the proton, the electron and the neutrino field. We shall work in the interaction picture. The tree level amplitude $\mathcal{A}$ is usually defined as

$$S_{FI} = I_{FI} + (2\pi)^4 i\delta^4(P_F^\mu - P_I^\mu)\mathcal{A}_{FI} = I_{FI} - i\left(\int d^4x H_I(x)\right)_{FI} \tag{9}$$

where the indices FI denote the matrix elements between the initial I and final state F, S is the S-matrix, I is the identity matrix and the Dirac delta enforces total 4-momentum conservation. For reasons that will become apparent in a moment, we work directly with the unnormalized matrix element $S_{FI} = i\left(\int d^4x H_I(x)\right)_{FI}$. Assuming, for simplicity, two neutrino flavors, the electron neutrino field can be written in terms of the mass neutrino fields as $\nu_e(x) = \cos\Theta\ \nu_1(x) + \sin\Theta\ \nu_2(x)$, with mixing angle Θ. The initial and final states for the inverse beta decay are

$$|I\rangle = |0_e\rangle\,|0_p\rangle\,|n_{P_n,s_n}\rangle\,|\nu_{e;P_\nu,s_\nu}(I)\rangle\ , \qquad |F\rangle = |e_{P_e,s_e}\rangle\,|p_{P_p,s_p}\rangle\,|0_n\rangle\,|0_\nu(F)\rangle \tag{10}$$

where the P_j are momentum indices, the s_j spin indices for $j = e, n, p, \nu$ and the tensor product is understood. The arguments I, F in the neutrino states are inserted to keep track of the two asymptotic limits $t_{I,F} \to \mp\infty$.

The difference in the various approaches to neutrino mixing is essentially in the definition of the neutrino flavor states. We distinguish four cases:

1. *Decoupled Pontecorvo states*
This is the case considered in the Ref. [34]. The neutrinos are originally produced as Pontecorvo flavor states $|\nu_e\rangle = \cos\Theta|\nu_1\rangle + \sin\Theta|\nu_2\rangle$ but are quickly decoupled due to the different propagation velocities for ν_1 and ν_2. At the observation time, these states have completely decohered into mass eigenstates, and the inverse beta decay takes the form, $\nu_j + n \to e^- + p$. For the effects of decoherence on neutrino oscillations see also ref. [42]. The only effect of mixing is in the interaction Hamiltonian (8), where the mixing matrix determines the fractions of ν_1 and ν_2 that interact as electron neutrinos. It is important to remark that in this case the neutrinos are mixed only at the level of states.
2. *Pontecorvo states*
In this case neutrinos are not only produced, but also interact as Pontecorvo flavor states. The mixing is to be understood at the level of fields $\nu_e(x) = \cos\Theta\ \nu_1(x) + \sin\Theta\ \nu_2(x)$ and is therefore "eternal" (no decoherence). The neutrino states entering the amplitude (9) are of the form $|\nu_e\rangle = \cos\Theta|\nu_1\rangle + \sin\Theta|\nu_2\rangle$. Such a definition neglects the spinorial nature of the neutrino states and amounts to the action of the flavor creation operator $a_e^\dagger = \cos\Theta\ a_1^\dagger + \sin\Theta\ a_2^\dagger$ on the neutrino vacuum state $|0_\nu\rangle$.
3. *Pontecorvo-Dirac states*
Also in this case mixing is at the level of fields. Here one does not neglect the spinorial nature of the neutrino states and sets $a_e^\dagger = (u_1, \nu_e(x))^\dagger \sim \cos\Theta a_1^\dagger + \sin\Theta\ U a_2^\dagger + \sin\Theta\ V b_2$, with $(,)$ denoting the Dirac inner product and b_2 the anti-ν_2 destruction operator. The coefficients U and V are the scalar products $U \sim (u_1, u_2), V \sim (u_1, v_2)$. When acting on the neutrino vacuum, the creation operator $a_e^\dagger$ produces the state $|\nu_e\rangle = \cos\Theta\ \ |\nu_1\rangle + \sin\Theta\ \ U|\nu_2\rangle$. This assumes a unique neutrino vacuum state, the mass vacuum $|0_\nu\rangle \equiv |0_M\rangle$ annihilated by a_1, a_2, b_1, b_2. Notice that in this case, since the flavor vacuum and the mass vacuum coincide $|0_F(t)\rangle = |0_M\rangle$, then

$$N^F_{\boldsymbol{k},i} = \langle 0_M|\, a^\dagger_{\boldsymbol{k},i} a_{\boldsymbol{k},i}\, |0_M\rangle = 0\ , \tag{11}$$

and the corresponding vacuum energy is equal to zero. One can also compute the expectation value of the operator $a^\dagger_{\boldsymbol{k},\sigma} a_{\boldsymbol{k},\sigma}$, with $\sigma = e, \mu$, on the vacuum state and to obtain, $\Upsilon^F_{\boldsymbol{k},i} = \langle 0_M|\, a^\dagger_{\boldsymbol{k},\sigma} a_{\boldsymbol{k},\sigma}\, |0_M\rangle = \sin^2\Theta|V_{\boldsymbol{k}}|^2$. This result analytically coincides with Eq. (4). However, the physical interpretation of $\Upsilon^F_{\boldsymbol{k},i}$ is completely different from that of the vacuum condensate density given in Eq. (4). Indeed, $\Upsilon^F_{\boldsymbol{k},i}$ is not related to the energy momentum tensor for free massive fields and its contribution to the energy of the universe is equal to zero. The vacuum energy (5), (and the corresponding in curved space (7)), is due only to the unitarily inequivalence of the mass and flavor representation of the Fock spaces in the infinite volume limit, that for Pontecorvo-Dirac states is absent, since the flavor Hilbert space H_f coincides with the Hilbert space for massive field H_m.

Table 1
Summary of the mixing schemes.

Case	$\cos\Theta/\sin\Theta$	$\cos\Psi/\sin\Psi$	U	V	N^F, ρ
Decoupled Pontecorvo	$\cos\Theta/\sin\Theta$	$\to 1/1$	1	0	0
Pontecorvo	$\cos\Theta/\sin\Theta$	$\cos\Theta/\sin\Theta$	1	0	0
Pontecorvo-Dirac	$\cos\Theta/\sin\Theta$	$\cos\Theta/\sin\Theta$	$\neq 1$	$\neq 0$	0
Flavor Fock space	$\cos\Theta/\sin\Theta$	$\cos\Theta/\sin\Theta$	$\neq 1$	$\neq 0$	$\neq 0$

4. *Flavor Fock space states*
The mixing is at the level of fields and no decoherence occurs. The flavor creation operator is again given by $a_e^\dagger \sim \cos\Theta a_1^\dagger + \sin\Theta\, U a_2^\dagger + \sin\Theta\, V b_2$, but in this case the flavor state is defined by its application on the *flavor vacuum* $|0_{\nu,f}\rangle$ which is distinct from the mass vacuum $|0_\nu\rangle$. The flavor vacuum $|0_{\nu,f}(t)\rangle$ depends explicitly on time t, whence the necessity of the I, F arguments in Eq. (10).

Only the last case features a condensed flavor vacuum, so that only in this case one has a dark matter contribution from the vacuum of the theory. Mathematically speaking the last case is the most general, as all the others can be obtained by taking the appropriate limits. To exhibit the relevant limits we distinguish the mixing matrix elements in the field $\nu_e = \cos\Theta\nu_1 + \sin\Theta\nu_2$ from those appearing in the definition of the states $|\nu_e\rangle \sim \cos\Psi|\nu_1\rangle + \sin\Psi|\nu_2\rangle$. When both are present, of course, $\Theta = \Psi$. The four cases can then be classified according to the Table 1. The last column is there referred to the condensation density $N^F_{\boldsymbol{k},i}$ and the energy density ρ associated to the flavor vacuum.

Since all the mixing schemes descend from the flavor Fock space approach in the appropriate limits, we compute the amplitude of eq. (9) and the corresponding cross section in this approach.

4. Amplitude and cross section

The object of interest is the unnormalized amplitude

$$S_{FI}(T) = -i\left(\int_{-\frac{T}{2}}^{\frac{T}{2}} dx^0 \int d^3x H_I(x)\right)_{FI} \tag{12}$$

where we have split off the time and space integrals. The integration boundary T is to be pushed to ∞, but we keep it finite, for the moment, for the sake of clarity. In general, we cannot extract a single δ^4 term from Eq. (12) due to the presence of terms with different energies. Using the generic states of Eq. (10) we can write

$$\begin{aligned} S_{FI}(T) = &-i\frac{G_F}{\sqrt{2}}\int_{-\frac{T}{2}}^{\frac{T}{2}} dx^0 \int d^3x\, V_{ud}\, \eta_{\alpha\beta}\, \langle p_{P_p,s_p}|\,\bar{p}(x)\,|0_p\rangle \left[\gamma^\alpha\left(f - g\gamma^5\right)\right]\langle 0_n|\,n(x)\,|n_{P_n,s_n}\rangle \\ &\times \langle e_{P_e,s_e}|\,\bar{e}(x)\,|0_e\rangle\left[\gamma^\beta\left(1-\gamma^5\right)\right]\langle 0_{\nu,f}(t_F)|\,\nu_e(x)\,|\nu_{e;P_\nu,s_\nu}(t_I)\rangle\ . \end{aligned} \tag{13}$$

The matrix elements of the neutron, the proton and the electron states are computed straightforwardly. As anticipated, the neutrino matrix element involves two (in principle distinct) time arguments t_I, t_F for the asymptotic states, due to the intrinsic time dependence of the flavor vacuum. The neutrino field is expanded as

$$\nu_e(x) = \sum_{r_\nu}\int \frac{d^3k}{\sqrt{(2\pi^3)}}\left[u^{r_\nu}_{\boldsymbol{k}_\nu;1} a^{r_\nu}_{\boldsymbol{k}_\nu;e}(x^0) + v^{r_\nu}_{-\boldsymbol{k}_\nu;1} b^{r_\nu\dagger}_{-\boldsymbol{k}_\nu;e}(x^0)\right] e^{i\boldsymbol{k}_\nu\cdot\boldsymbol{x}} \tag{14}$$

where the spinors are normalized to $u_j^\dagger u_j = 2E_{\nu;j} = 2\sqrt{\boldsymbol{k}_\nu^2 + m_j^2}$ and boldface letters are used to denote spatial 3-vectors. By definition the flavor operators are

$$\begin{aligned} a^s_{\boldsymbol{k},\nu_e}(x^0) &= e^{-iE_{\nu;1}x^0}\left[\cos\Theta a^s_{\boldsymbol{k},1} + \sin\Theta\left(U^*_{\boldsymbol{k}}(x^0) a^s_{\boldsymbol{k},2} + \epsilon^s V_{\boldsymbol{k}}(x^0) b^{s\dagger}_{-\boldsymbol{k},2}\right)\right] \\ b^s_{-\boldsymbol{k},\nu_e}(x^0) &= e^{-iE_{\nu;1}x^0}\left[\cos\Theta b^s_{-\boldsymbol{k},1} + \sin\Theta\left(U^*_{\boldsymbol{k}}(x^0) b^s_{-\boldsymbol{k},2} - \epsilon^s V_{\boldsymbol{k}}(x^0) a^{s\dagger}_{\boldsymbol{k},2}\right)\right] \end{aligned}$$

where we have assumed, without loss of generality, the neutrino momentum $\boldsymbol{k}_\nu$ along the third axis and $\epsilon^s = (-1)^{s-\frac{1}{2}}$ for spin projections $s = \pm\frac{1}{2}$. The Bogoliubov coefficients are $U_{\boldsymbol{k}}(x^0) = |U_{\boldsymbol{k}}|e^{i(E_{\nu;2}-E_{\nu;1})x^0}$, $V_{\boldsymbol{k}}(x^0) = |V_{\boldsymbol{k}}|e^{i(E_{\nu;2}+E_{\nu;1})x^0}$ with $|U_{\boldsymbol{k}}|, |V_{\boldsymbol{k}}|$ given in the references [23–25].

As it stands, with distinct time arguments t_I, t_F, the neutrino matrix element cannot be computed straightforwardly for the following reasons:

- The difference between t_I and t_F would take into account the intrinsic oscillation properties of the flavor Fock space states (including the vacuum), which is not appropriate for the evaluation of a scattering amplitude. The "asymptotic" neutrino states should not involve oscillations at times before and after the interaction process.

- The flavor states at times t_I and t_F belong to mutually orthogonal Hilbert spaces if $t_I \neq t_F$, due to the unitary inequivalence of the Flavor Fock spaces at distinct times (see also appendix B). The matrix elements $\langle 0_{\nu,f}(t_I)|\, \nu_e(x)\, |\nu_{e;P_\nu,s_\nu}(t_F)\rangle$ vanish for $t_I \neq t_F$. The in-out formalism then cannot be applied, unless one considers the limit $t_F \to t_I$.

In any case, due to the small timescales of the weak interaction, it is reasonable to consider the approximation $t_F \simeq t_I$. We then set $t_F = t_I$ and assume $t_F = t_I = 0$. The neutrino matrix element can now be computed easily (omitting the t_I/t_F time arguments)

$$
\begin{aligned}
&\langle 0_{\nu,f}|\, \nu_e(x)\, |\nu_{e;P_\nu,s_\nu}\rangle = \\
&\sum_{r_\nu} \int \frac{d^3k_\nu}{\sqrt{2\pi}^3} e^{i\boldsymbol{k}_\nu\cdot \boldsymbol{x}} \left[u^{r_\nu}_{\boldsymbol{k}_\nu;1} \langle 0_{\nu,f}| \left\{ a^{r_\nu}_{\boldsymbol{k}_\nu;\nu_e}(x^0), a^{s_\nu\dagger}_{\boldsymbol{p}_\nu;\nu_e} \right\} |0_{\nu,f}\rangle + v^{r_\nu}_{-\boldsymbol{k}_\nu;1} \langle 0_{\nu,f}| \left\{ b^{r_\nu\dagger}_{-\boldsymbol{k}_\nu;\nu_e}(x^0), a^{s_\nu\dagger}_{\boldsymbol{p}_\nu;\nu_e} \right\} |0_{\nu,f}\rangle \right] = \\
&\frac{e^{i\boldsymbol{p}_\nu\cdot \boldsymbol{x}}}{\sqrt{2\pi}^3} \Bigg[u^{s_\nu}_{\boldsymbol{p}_\nu;1} \left(\cos\Theta \cos\Psi e^{-iE_{\nu;1}x^0} + \sin\Theta\sin\Psi \left(|U_{\boldsymbol{p}_\nu}|^2 e^{-iE_{\nu;2}x^0} + |V_{\boldsymbol{p}_\nu}|^2 e^{iE_{\nu;2}x^0} \right) \right) \\
&+ v^{s_\nu}_{-\boldsymbol{p}_\nu;1} \epsilon^{s_\nu} \sin\Theta \sin\Psi |U_{\boldsymbol{p}_\nu}||V_{\boldsymbol{p}_\nu}| \left(e^{-iE_{\nu;2}x^0} - e^{iE_{\nu;2}x^0} \right) \Bigg]
\end{aligned} \tag{15}
$$

where we have kept the notation Θ, Ψ to distinguish the mixing angles in the field and in the states. Notice that in Eq. (15) the mixing angle appears both due the electron neutrino state $|\nu_{e,P_\nu,s_\nu}\rangle$ and due to the electron neutrino field $\nu_e(x)$.[2]

Inserting the neutrino matrix element in Eq. (13) and taking the infinite time limit $T \to \infty$ we find

$$
S_{FI} = \delta^4(p^\mu_n + p^\mu_{\nu,1} - p^\mu_p - p^\mu_e) M_{\nu_1} + \delta^4(p^\mu_n + p^\mu_{\nu,2} - p^\mu_p - p^\mu_e) M_{\nu_2} + \delta^4(p^\mu_n + \bar{p}^\mu_{\nu,2} - p^\mu_p - p^\mu_e) M_{\bar{\nu}_2}\,, \tag{16}
$$

where $p^\mu_{\nu,j} \equiv (E_{\nu;j}, \boldsymbol{p}_\nu)$, $\bar{p}^\mu_{\nu,j} \equiv (-E_{\nu;j}, \boldsymbol{p}_\nu)$ and

$$
\begin{aligned}
&M_{\nu_1} = -\frac{G_F}{\sqrt{2}} V_{ud}\eta_{\alpha\beta} \cos\Theta\cos\Psi R^{\alpha\beta}_1\,; \quad M_{\nu_2} = -\frac{G_F}{\sqrt{2}} V_{ud}\eta_{\alpha\beta} \sin\Theta\sin\Psi R^{\alpha\beta}_2\,; \quad M_{\bar{\nu}_2} = -\frac{G_F}{\sqrt{2}} V_{ud}\eta_{\alpha\beta} \sin\Theta\sin\Psi \epsilon^{s_\nu} L^{\alpha\beta}_2 \\
&R^{\alpha\beta}_j = \bar{u}^{s_p}_{\boldsymbol{p}_p} \gamma^\alpha (f - g\gamma^5) u^{s_n}_{\boldsymbol{p}_n} \bar{u}^{s_e}_{\boldsymbol{p}_e} \gamma^\beta (1-\gamma^5) u^{s_\nu}_{\boldsymbol{p}_\nu,j} \qquad L^{\alpha\beta}_j = \bar{u}^{s_p}_{\boldsymbol{p}_p} \gamma^\alpha (f - g\gamma^5) u^{s_n}_{\boldsymbol{p}_n} \bar{u}^{s_e}_{\boldsymbol{p}_e} \gamma^\beta (1-\gamma^5) v^{s_\nu}_{-\boldsymbol{p}_\nu,j}\,.
\end{aligned}
$$

The amplitude of Eq. (16) has the form of Eq. (A.2) in the infinite volume and infinite time limits. The cross section is then defined according to Eq. (A.5). In computing the squared amplitudes $|M|^2$, we specialize to the neutron rest frame and neglect the proton recoil [34], so that the 4-momenta are $p^\mu_n \equiv (m_n, 0)$, $p^\mu_p \simeq (m_p, 0)$, $p^\mu_e \equiv (E_e, \boldsymbol{p}_e)$, $p^\mu_{\nu,j} \equiv (E_{\nu,j}, \boldsymbol{p}_\nu)$. We also set $\boldsymbol{p}_e \cdot \boldsymbol{p}_\nu = p_e p_\nu \cos\theta$, sum over the neutron and proton spins and average over the electron spin, in order to get the unpolarized cross section. Then

$$
\begin{aligned}
|M_{\nu_1}|^2 &= 8G_F^2 |V_{ud}|^2 \cos^2\Theta \cos^2\Psi m_p m_n E_e E_{\nu,1} \left[(1 - 2s_\nu v_\nu)(3g^2 + f^2) + (v_\nu - 2s_\nu)(f^2 - g^2) v_e \cos\theta \right] \\
|M_{\nu_2}|^2 &= 8G_F^2 |V_{ud}|^2 \sin^2\Theta \sin^2\Psi |U_{\boldsymbol{p}_\nu}|^2 m_p m_n E_e E_{\nu,2} \left[(1 - 2s_\nu v_\nu)(3g^2 + f^2) + (v_\nu - 2s_\nu)(f^2 - g^2) v_e \cos\theta \right] \\
|M_{\bar{\nu}_2}|^2 &= 8G_F^2 |V_{ud}|^2 \sin^2\Theta \sin^2\Psi |V_{\boldsymbol{p}_\nu}|^2 m_p m_n E_e E_{\nu,2} \left[(1 - 2s_\nu v_\nu)(3g^2 + f^2) + (v_\nu - 2s_\nu)(f^2 - g^2) v_e \cos\theta \right]
\end{aligned} \tag{17}
$$

where we have introduced the velocities $v_j = \frac{p_j}{E_j}$. The first and the second of the squared amplitudes of Eq. (17) agree with those obtained in [34] except for the factors in Ψ and $|U_{\boldsymbol{p}_\nu}|$. The interpretation of the last term in Eqs. (16) and (17) requires more care. The second delta function in Eq. (16) forces the energy conservation as $E_{\nu,2} = E_p + E_e - E_n (> 0)$, but the third delta function involves the opposite sign of the neutrino energy, enforcing $E_{\nu,2} = -(E_p + E_e - E_n)$. Assuming the same electron, proton and neutron energies, the last delta implies a negative energy $E_{\nu,2} = -|E_{\nu,2}| (< 0)$.

We acknowledge two possibilities for the third term:

- If strictly interpreted as the neutrino energy, this term must be discarded, since by definition only positive energies are possible. This is also the route followed in the Ref. [38] in computing the beta decay spectrum. Discarding the last term is equivalent to set $V_{\boldsymbol{p}_\nu} = 0$, so that one obtains the same result as for the Pontecorvo-Dirac states (see Table 1).
- If interpreted within the context of the condensate structure of the flavor states, the negative energy $-|E_{\nu,2}|$ may be viewed as the energy associated with a ν_2 “hole” in the condensate. This is the kind of reasoning invoked in [43]. The last term is then retained with a change of sign in the energy $E_{\nu,2}$ with respect to the second term. Assuming a negative energy for the third term brings both the second and third delta functions to the form $\delta(E_n + |E_{\nu,2}| - E_e - E_p)$. It is worth noting that the third term $\delta(E_n - E_{\nu,2} - E_p - E_e)\delta^3(\boldsymbol{p}_n + \boldsymbol{p}_\nu - \boldsymbol{p}_p - \boldsymbol{p}_e)|M_{\bar{\nu}_2}|^2$ also admits another interpretation. Both the delta function and the amplitude (apart from a $\sin^2\Psi|V_{\boldsymbol{p}_\nu}|$ factor) may be considered to describe the decay $n \to e^- + p + \bar{\nu}_2$ for an antineutrino $\bar{\nu}_2$ with (positive) energy $E_{\nu,2}$ and momentum $-\boldsymbol{p}_\nu$. If interpreted in this way, the amplitude of Eq. (16) is a (weighed) superposition of the amplitudes for three processes, inverse beta decay for ν_1 and ν_2 and a direct beta decay for $\bar{\nu}_2$. The condensate structure of the flavor states is such that the absorption of a ν_2 and the emission of a $\bar{\nu}_2$ are combined to yield the ν_e inverse beta decay amplitude.

[2] It is also important to stress that only the electron neutrino takes part into the inverse beta decay, independently from the definition adopted for the electron neutrino state. Let n_ν be the number density of neutrinos per degree of freedom, which we assume to be the same for the two flavors e and μ. Neutrino oscillations do not alter the expected number density of electron neutrinos at detection. Electron neutrinos do indeed come from neutrinos originally produced as electron neutrinos which have survived with probability $P_{e\to e}$ and from neutrinos originally produced as muon neutrinos which have oscillated into electron neutrinos with probability $P_{\mu\to e} = 1 - P_{e\to e}$. The expected number density of electron neutrinos at detection is then $n_\nu(P_{e\to e} + P_{\mu\to e}) = n_\nu$, which is clearly the same as in absence of oscillations. Therefore oscillations do not alter the capture rate resulting from the amplitude (15) and the terms depending on the mixing angle survive in the capture cross section of Eq. (23) as shown below.

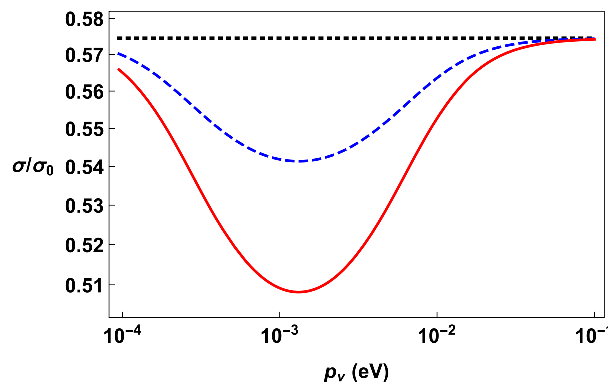

Fig. 1. Plot of the ratio $\frac{\sigma(p_\nu)}{\sigma_0}$ as a function of the neutrino momentum p_ν in the range $[10^{-4}, 10^{-1}]$ eV. The black dotted line corresponds to the Pontecorvo cross section (Eq. (25)) $\sigma(p_\nu) = \sigma_P$; the blue dashed line is the Pontecorvo-Dirac cross section (Eq. (26) $\sigma(p_\nu) = \sigma_{PD}$, and the red solid line is the flavor Fock space cross section (Eq. (27)) $\sigma(p_\nu) = \sigma_F$. The ratio of the cross section for decoupled neutrinos $\frac{\sigma_0}{\sigma_0}$ is 1 by definition, and has not been plotted. The parameters have been chosen as $\sin^2\Theta = \sin^2\Theta_{12} = 0.307$, $\Delta m^2 = \Delta m^2_{12} = 7.53 \times 10^{-5}$ eV^2 and $m_1 = 2 \times 10^{-4}$ eV.

From the formula (A.5), having for the Mandelstam variables, $s \simeq m_n^2, t \simeq (m_e - m_\nu)^2 + 2p_e p_\nu \cos\theta$, we can write the differential cross section as

$$\begin{aligned}\frac{d\sigma}{d\cos\theta} &= \frac{1}{32\pi}\frac{1}{m_n^2}\frac{p_e}{p_\nu}\left[|M_{\nu_1}|^2(E_{\nu,1}) + |M_{\nu_2}|^2(|E_{\nu,2}|) + |M_{\bar{\nu}_2}|^2(-|E_{\nu,2}|)\right] \\ &= \frac{G_F^2}{4\pi}|V_{ud}|^2\frac{m_p E_e p_e}{m_n}\Bigg[\Big(A_1(s_\nu)(f^2+3g^2) + B_1(s_\nu)(f^2-g^2)v_e\cos\theta\Big)\frac{\cos^2\Theta\cos^2\Psi}{v_{\nu,1}} \\ &+ \Big(A_2(s_\nu)(f^2+3g^2) + B_2(s_\nu)(f^2-g^2)v_e\cos\theta\Big)\frac{\sin^2\Theta\sin^2\Psi|U_{\boldsymbol{p}_\nu}|^2}{v_{\nu,2}} \\ &- \Big(A_{\bar{2}}(s_\nu)(f^2+3g^2) + B_{\bar{2}}(s_\nu)(f^2-g^2)v_e\cos\theta\Big)\frac{\sin^2\Theta\sin^2\Psi|V_{\boldsymbol{p}_\nu}|^2}{v_{\nu,2}}\Bigg]. \end{aligned} \tag{18}$$

Here we have explicitly written the neutrino energy argument in order to keep track of the change of sign in the last term. The functions A and B are defined as

$$A_j(s_\nu) = 1 - 2s_\nu v_{\nu,j}, \tag{19}$$

$$B_j(s_\nu) = v_{\nu,j} - 2s_\nu, \tag{20}$$

$$A_{\bar{j}}(s_\nu) = 1 + 2s_\nu v_{\nu,j}, \tag{21}$$

$$B_{\bar{j}}(s_\nu) = -v_{\nu,j} - 2s_\nu, \tag{22}$$

in terms of the (positive) neutrino velocities $v_{\nu,j} = \frac{p_\nu}{|E_{\nu,j}|}$. Notice the change of sign in $A_{\bar{j}}, B_{\bar{j}}$ prompted by the substitution $|E_\nu| \to -|E_\nu|$. The integral over $\cos\theta$ is trivial and cancels all the B terms. For the nonrelativistic neutrinos considered here $v_{\nu,j} = \frac{p_{\nu,j}}{E_{\nu,j}} \ll 1$, so that $A_j(s_\nu) = A_{\bar{j}}(s_\nu) \to 1$ and we can neglect the difference $v_{\nu,1} - v_{\nu,2} = \frac{p_\nu(m_2-m_1)}{m_1 m_2} \ll 1$. We then multiply Eq. (18) by, $v_{\nu,1} \simeq v_{\nu,2}$, and the Fermi function, $F(Z, E_e) = \frac{2\pi\eta}{1-e^{-2\pi\eta}}$, with $\eta = \alpha\frac{E_e}{p_e}$, to obtain the capture cross section

$$\sigma = \frac{G_F^2}{2\pi}|V_{ud}|^2 F(Z,E)\frac{m_p E_e p_e}{m_n}(f^2+3g^2)\left[\cos^2\Theta\cos^2\Psi + \sin^2\Theta\sin^2\Psi\left(|U_{\boldsymbol{p}_\nu}|^2 - |V_{\boldsymbol{p}_\nu}|^2\right)\right]. \tag{23}$$

This equation represents the most general form for the capture cross section. The term in square brackets includes the mixing angles and the Bogoliubov coefficients because of the structure of Eq. (15).

Two points need here to be remarked. The first concerns the velocity factor v_ν by which we multiply to obtain the capture cross section. For definiteness this corresponds to the lightest neutrino mass, i.e. $v_{\nu,1} = \frac{p_\nu}{E_{\nu,1}} \ll 1$. By assumption the neutrinos considered are very nonrelativistic, i.e. $\frac{p_\nu}{m_{\nu,j}} \ll 1$. We then make a vanishingly small error in neglecting the difference between the two neutrino velocities, since $v_{\nu,1} - v_{\nu,2} \simeq \frac{p_\nu(m_2-m_1)}{m_1 m_2} \ll 1$. For instance, for $p_\nu = 10^{-4}$ eV and $m_{\nu,1} = 10^{-2}$ eV, the difference is of order $v_{\nu,1} - v_{\nu,2} \simeq 10^{-3}$. While in principle each of the terms appearing in Eq. (25) should be multiplied by the corresponding neutrino velocity, this only brings along a vanishingly small correction. The second remark concerns the capture cross section of Eq. (23) and depicted in Fig. 1. By definition this is given by the product of the cross section and the neutrino velocity. It is customary to employ the so defined capture cross section, instead of the usual cross section, for convenience (see e.g. [34]). The capture cross sections do indeed include a velocity factor which allows to define the capture rate as in Eq. (28) without any additional velocity factor. The neutrino velocity must appear as part of the definition of the neutrino flux in the capture rate, independently of the definition adopted for the cross section. Then if one employs the standard definition of the cross section, in place of the capture cross section, the capture rate must involve an additional velocity term in its definition. Of course the two definitions for the observable capture rate of Eq. (28) are identical, and it is only a matter of convention where to put the velocity factor (either defining the capture cross section or directly in the capture rate).

We can now give an explicit expression for the capture cross section in the various schemes summarized in Table 1. Recall that, mathematically, the Flavor Fock space approach represents the most general case, as all the other cases can be deduced by discarding some of the terms, as summarized in Table 1. For instance, the capture cross section for the Pontecorvo-Dirac case can be obtained from the corresponding result in the Flavor Fock space approach, Eq. (23), by simply putting $V_{\boldsymbol{k}} = 0$. The capture cross section for the various mixing schemes summarized in Table 1 is then:

1. *Decoupled Pontecorvo*
   Unsurprisingly, the cross section in this case matches the result of Ref. [34]
   $$\sigma_0 = \frac{G_F^2}{2\pi}|V_{ud}|^2 F(Z,E)\frac{m_p E_e p_e}{m_n}(f^2+3g^2)\,, \tag{24}$$
   showing that Eq. (23) constitutes a proper generalization.
2. *Pontecorvo*
   Here $U \to 1$, $V \to 0$ and $\Psi \to \Theta$ and the cross section reads
   $$\sigma_P = \frac{G_F^2}{2\pi}|V_{ud}|^2 F(Z,E)\frac{m_p E_e p_e}{m_n}(f^2+3g^2)\left[\cos^4\Theta + \sin^4\Theta\right]\,. \tag{25}$$
   We can see that the difference with respect to the first case is only in the multiplicative factor, $\cos^4\Theta + \sin^4\Theta$.
3. *Pontecorvo-Dirac*
   The cross section has a non-trivial dependence on the neutrino momentum via $|U_{\boldsymbol{p}_\nu}|$:
   $$\sigma_{PD} = \frac{G_F^2}{2\pi}|V_{ud}|^2 F(Z,E)\frac{m_p E_e p_e}{m_n}(f^2+3g^2)\left[\cos^4\Theta + \sin^4\Theta|U_{\boldsymbol{p}_\nu}|^2\right]\,. \tag{26}$$
   Recall that the same result is obtained within the flavor Fock space approach if the negative energy term is discarded.
4. *Flavor Fock space states*
   For the cross section we have
   $$\sigma_F = \frac{G_F^2}{2\pi}|V_{ud}|^2 F(Z,E)\frac{m_p E_e p_e}{m_n}(f^2+3g^2)\left[\cos^4\Theta + \sin^4\Theta\left(|U_{\boldsymbol{p}_\nu}|^2 - |V_{\boldsymbol{p}_\nu}|^2\right)\right]\,. \tag{27}$$
   This result is acceptable if the negative energy term is interpreted as a condensate hole term, otherwise one gets Eq. (26).

The capture cross sections of Eqs. (24), (25), (26) and (27) refer to the neutrino capture on a free neutron. In order to obtain the capture cross sections on tritium $\nu_e + {}^3\mathrm{H} \to {}^3\mathrm{He} + e^-$, all these expressions have to be changed according to the procedure described in the ref. [34]. In particular, the nucleon masses m_n, m_p are replaced with the masses of the atomic species $m_{^3\mathrm{H}}$ and $m_{^3\mathrm{He}}$, the form factors $f^2, 3g^2$ are replaced with the nuclear matrix elements $\langle f_F\rangle^2, (g_A/g_V)^2\langle g_{GT}\rangle^2$, and the electron kinetic energy $E_e - m_e$ must be modified accordingly. Let us set, for convenience

$$\sigma_{n0} = \frac{G_F^2}{2\pi}|V_{ud}|^2 F(Z,E)\frac{m_p E_e p_e}{m_n}(f^2+3g^2)$$
$$\sigma_{T0} = \frac{G_F^2}{2\pi}|V_{ud}|^2 F(Z,E)\frac{m_{^3\mathrm{He}} E_e p_e}{m_{^3\mathrm{H}}}(\langle f_F\rangle^2 + (g_A/g_V)^2\langle g_{GT}\rangle^2)$$

denoting, respectively, the capture cross sections for decoupled neutrinos on free neutrons σ_{n0} (Eq. (24)) and on tritium σ_{T0}. Notice that the ratios between the cross section in a given scheme $\sigma = \sigma_P$ (Pontecorvo), σ_{PD} (Pontecorvo-Dirac), σ_F (Flavor Fock space), and the reference cross section for decoupled neutrinos σ_0 are the same for the capture on free neutrons and on tritium, i.e. $\frac{\sigma_{n\alpha}}{\sigma_{n0}} = \frac{\sigma_{T\alpha}}{\sigma_{T0}}$ for each $\alpha =$ P, PD, F. The ratios are plotted in Fig. 1 for neutrino momenta p_ν in the range $[10^{-4}, 10^{-1}]$ eV.

The capture rate on a sample of tritium of mass M_S can be expressed in terms of the capture cross section σ as

$$d\Gamma = \sigma N_T dn_\nu\,, \tag{28}$$

where $N_T = \frac{M_S}{m_{^3\mathrm{He}}}$ is the total number of tritium nuclei in the sample and dn_ν is the (differential) number density of neutrinos per degree of freedom. Notice that the definition of Eq. (28) does not include explicitly the velocity of neutrinos, which is part of the neutrino flux. This is because the neutrino velocity is already included implicitly in the definition of the capture cross section σ. Within the sudden freeze-out approximation, the phase space distribution of neutrinos is the redshifted distribution function that was realized at the decoupling epoch. At redshift z, the number density reads

$$dn_\nu(z) = \frac{d^3p(z)}{(2\pi)^3}\frac{1}{e^{\frac{p(z)}{T_\nu(z)}}+1} = \frac{p^2(z)dp(z)}{2\pi^2}\frac{1}{e^{\frac{p(z)}{T_\nu(z)}}+1} \tag{29}$$

where we have performed the solid angle integration in the last step. Here, $p(z) = \frac{1+z}{1+z_{FO}}p_{FO}$, $T_\nu(z) = \frac{1+z}{1+z_{FO}}T_{\nu,FO}$ and $z_{FO} = 6\times 10^{10}$, [34] with the label FO denoting the quantities at the freeze-out. We remark that in principle the distribution of Eq. (29) should involve

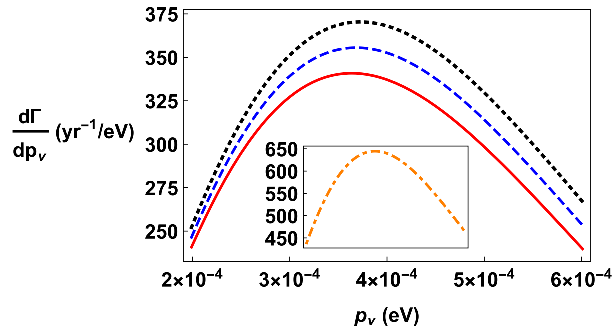

Fig. 2. Plot of the differential capture rate (Eq. (31)) $\frac{d\Gamma(p_\nu)}{dp_\nu}$ as a function of the neutrino momentum p_ν in the range $[2\times10^{-4}, 6\times10^{-4}]$ eV. The differential rate is of course adimensional, but is expressed in terms of $\mathrm{yr}^{-1}/\mathrm{eV}$ for ease of comparison with the previous results. The black dotted line corresponds to the Pontecorvo cross section (Eq. (25)) $\sigma(p_\nu)=\sigma_P$, the blue dashed line is the Pontecorvo-Dirac cross section (Eq. (26) $\sigma(p_\nu)=\sigma_{PD}$ and the red solid line is the Flavor Fock space cross section (Eq. (27)) $\sigma(p_\nu)=\sigma_F$. In the inset we plot the capture rate (orange dotdashed line) corresponding to the decoupled Pontecorvo cross section (Eq. (24)). We have assumed a sample of tritium with total mass $M_S = 100$ g. The other parameters have been chosen as in figure 1.

the neutrino energies $E_{\nu,j}$ in place of the momentum p_ν. However the temperature at the freeze-out $T_{\nu,FO}$ is much higher than the neutrino masses $m_{\nu,j}$, so that the latter are usually neglected [34,44], so that $E_{\nu,j}\simeq p_\nu$. We point out that we are analyzing the neutrino capture process which takes place in the present epoch. Therefore all the effects of neutrino propagation prior to the capture process are neglected, including the ones regarding the early universe. The only effect of the universe evolution on the process is in the appearance of the redshifted momentum in the distribution of Eq. (29). Besides the momentum redshift, the evolution of the universe may have an impact in the form of kinematic decoherence if the initial mass states are not plane waves but generic wave packets. This kind of decoherence would of course affect all the states considered (Decoupled Pontecorvo, Pontecorvo, Pontecorvo-Dirac and Flavor Fock space approach) and then affect also the corresponding capture rate. The influence of kinematical decoherence is the same for all the approaches, and therefore the differential capture rate $\frac{d\Gamma}{dp_\nu}$, remains different for the different approaches. Moreover the energy density ρ of (7), which is the expectation value of the energy-momentum tensor on the flavor vacuum is not affected by decoherence (the vacuum $|0_F\rangle$ is not affected by decoherence.). This means that even including the decoherence the neutrino capture on tritium can be used as a probe of flavor vacuum condensate and of dark matter. The study of the decoherence induced by the expansion of the universe lies beyond the scope of the present paper and will be studied in a future work. At the current epoch $z=0$ we have

$$dn_\nu(z=0) = dp_\nu \frac{p_\nu^2}{2\pi^2}\frac{1}{e^{\frac{p_\nu}{T_\nu}}+1} \tag{30}$$

where $p_\nu = p(z=0)$ and $T_\nu = T_\nu(z=0)\simeq 0.168\times10^{-3}$ eV. Finally, the differential capture rate becomes

$$\frac{d\Gamma}{dp_\nu} = N_T \frac{\sigma(p_\nu)p_\nu^2}{2\pi^2}\frac{1}{e^{\frac{p_\nu}{T_\nu}}+1} \tag{31}$$

with the capture cross section $\sigma(p_\nu)$. The capture rate of eq. (31) is twice as large for Majorana neutrinos [34]. In Fig. 2, we plot the differential capture rate for the various schemes discussed above.

As it is evident from Fig. 2, the capture rate for coupled neutrinos is smaller than the capture rate for decoupled neutrinos due to the factor $\cos^4\Theta + \sin^4\Theta < 1$. The dependence on the neutrino momentum is different for all the four cases considered, due to the presence (or the absence) of the Bogoliubov coefficients U and V. In particular, the capture rate for neutrinos is the lowest for the flavor Fock space states (the red line in Fig. 2). We remark that it is this last case that corresponds to the condensed flavor vacuum, and hence to a possible dark matter component. As anticipated, the difference between the various approaches is mostly relevant for neutrino momenta comparable to the neutrino masses $p_\nu \simeq m_\nu$. For larger momenta all the three curves of Fig. 2 converge to the Pontecorvo result (the black dotted line). A similar conclusion holds for the capture cross sections, as it can be seen from Fig. 1.[3] The overall size of the capture rate is set by the decoupled case, as all the other cases are of the same order of magnitude (as evident also in Fig. 2) and are smaller by a factor $\simeq \frac{1}{2}$. Estimates for the decoupled capture rate can be found in [34], and are, for the 100 g sample used in PTOLEMY [33], $\Gamma^M \simeq 8.12\ \mathrm{yr}^{-1}$ and $\Gamma^D \simeq 4.06\ \mathrm{yr}^{-1}$ respectively for Majorana and Dirac neutrinos. Clustering and neutrino mass hierarchy may affect this value, as discussed in [34]. However these effects are present for each of the cases considered in this work, and do only alter the overall size of the capture rate and capture cross section, leaving the ratios untouched.

It is convenient to spend a couple of words on the three-flavor generalization of our results. As before, we shall focus on the flavor Fock space approach, as all the other cases descend from it in the appropriate limits. The essential distinction with respect to the two-flavors setting comes from the definition of the flavor ladder operators, which now read [23]

[3] Equation (31) was obtained considering that the temperature at the freeze out $T_{\nu,FO}$ is much bigger than the neutrino masses. Considering the full expression Eq. (29) becomes

$$dn_\nu(z) = \frac{d^3p(z)}{(2\pi)^3}\frac{1}{e^{\frac{E(z)}{T_\nu(z)}}+1} = \frac{p^2(z)dp(z)}{2\pi^2}\frac{1}{e^{\frac{E(z)}{T_\nu(z)}}+1}$$

with $E(z) = \frac{1+z}{1+z_{FO}}E_{FO}$ and E_{FO} the neutrino energy at the freeze-out. In each case the qualitative behavior shown in Fig. 2 is preserved for the various cases. This is because the differences among the various cases considered are only due to the appearance of the Bogoliubov coefficients in the capture cross section.

$$a^s_{\boldsymbol{k},\nu_e}(t) == c_{12}c_{13}\, a^s_{\boldsymbol{k},1} + s_{12}c_{13}\left(U^*_{\boldsymbol{k};12}(t)a^s_{\boldsymbol{k},2} + \epsilon^s V_{\boldsymbol{k};12}(t)b^{s\dagger}_{-\boldsymbol{k},2}\right) + e^{-i\delta}s_{13}\left(U^*_{\boldsymbol{k};13}(t)a^s_{\boldsymbol{k},3} + \epsilon^s V_{\boldsymbol{k};13}(t)b^{s\dagger}_{-\boldsymbol{k},3}\right) .$$

Here $c_{ij} = \cos\theta_{ij}$, $s_{ij} = \sin\theta_{ij}$, δ is the Dirac CP-violating phase and the CKM parametrization of the mixing matrix has been assumed. The Bogoliubov coefficients have the same form as in Eq. (2), except that for any U_{ij}, V_{ij} one substitutes $m_1 \to m_i$ and $m_2 \to m_j$. Computing the capture amplitude one finds the same structure as in Eq. (16) with two extra terms

$$\delta^4(p^\mu_n + p^\mu_{\nu,3} - p^\mu_p - p^\mu_e)M_{\nu_3} + \delta^4(p^\mu_n + \bar{p}^\mu_{\nu,3} - p^\mu_p - p^\mu_e)M_{\bar{\nu}_3} .$$

This leads to the cross section (compare with (27))

$$\sigma_{3F} = \frac{G_F^2}{2\pi}|V_{ud}|^2 F(Z,E)\frac{m_p E_e p_e}{m_n}(f^2+3g^2)\left[c^4_{12}c^4_{13} + c^4_{13}s^4_{12}\left(|U_{\boldsymbol{p}_\nu;12}|^2 - |V_{\boldsymbol{p}_\nu;12}|^2\right) + s^4_{13}\left(|U_{\boldsymbol{p}_\nu;13}|^2 - |V_{\boldsymbol{p}_\nu;13}|^2\right)\right] . \tag{32}$$

We can read off the Pontecorvo-Dirac and the Pontecorvo equivalents as

$$\begin{aligned}
\sigma_{3PD} &= \frac{G_F^2}{2\pi}|V_{ud}|^2 F(Z,E)\frac{m_p E_e p_e}{m_n}(f^2+3g^2)\left[c^4_{12}c^4_{13} + c^4_{13}s^4_{12}|U_{\boldsymbol{p}_\nu;12}|^2 + s^4_{13}|U_{\boldsymbol{p}_\nu;13}|^2\right]\\
\sigma_{3P} &= \frac{G_F^2}{2\pi}|V_{ud}|^2 F(Z,E)\frac{m_p E_e p_e}{m_n}(f^2+3g^2)\left[c^4_{12}c^4_{13} + c^4_{13}s^4_{12} + s^4_{13}\right]
\end{aligned} \tag{33}$$

while the decoupled cross section is left unchanged $\sigma_{3,0} = \sigma_0$. Overall one has a much more involved momentum dependence in the cross sections. However they retain the same behavior as in the two flavor case. In particular, also for three flavors, they are lowered in going from the Pontecorvo states to the Pontecorvo-Dirac and the flavor Fock space states. Finally, the neutrino masses and their hierarchy may have important effects on the capture rate. It may happen, indeed, that some neutrino species ν_j may actually be relativistic, while others are not. This has an immediate impact on the capture rate. If the species j is relativistic $p \gg m_{\nu j} \to v_{\nu_j} \simeq 1$, the helicity factors in Eq. (18) become

$$\begin{aligned}
A_j(s_\nu) &= 1 - 2s_\nu ,\\
A_{\bar{j}}(s_\nu) &= 1 + 2s_\nu ,
\end{aligned}$$

so that one of the two helicities is necessarily suppressed, and one finds unequal rates for the capture of neutrinos with different spins. We point out that the behavior of the capture cross sections is already contemplated in their two-flavor expressions, and only minimal differences arise from the introduction of a third flavor. For completeness we now discuss another kind of neutrino condensate (neutrino superfluid) which has been analyzed in the literature.

4.1. A side on other neutrino condensates

The flavor condensate discussed above arises due to the inequivalence between the mass and flavor representations and is characterized as the vacuum state $|0_F(t)\rangle$ of the flavor Fock space. Nowhere in the construction of the flavor Fock space appears any interaction other than the neutrino mass terms that are responsible for mixing. Moreover, it is tacitly assumed that the construction is carried at zero temperature. There exists a different class of neutrino condensates, which is triggered by an effective attractive interaction between left-handed and right-handed (anti)-neutrinos, leading to a BCS-like condensate of neutrino pairs. These are also known as neutrino superfluids [50,51]. It is fundamental to stress that the appearance of neutrino superfluids requires an attractive interaction, usually due to the exchange of a scalar field (i.e. Higgs or a generalization thereof) of the form [50]

$$H_I = -\frac{h_\nu^2}{4m_\sigma^2}\left(2\nu^\dagger_{La}\nu^\dagger_{Rb}\nu_{Lb}\nu_{Ra} + \nu^\dagger_{La}\nu^\dagger_{Lb}\nu_{Rb}\nu_{Ra} + \nu^\dagger_{Ra}\nu^\dagger_{Rb}\nu_{Lb}\nu_{La}\right) . \tag{34}$$

Here the spinor components are explicitly indicated by a, b, the indices L, R label the left-handed and right-handed fields, m_σ is the Higgs mass and h_ν is the Yukawa coupling to the Higgs. The interaction of Eq. (34) is written for a single Dirac neutrino field, but a similar expression holds for Majorana fields [51], provided that the field labels are appropriately modified to take into account the Majorana nature. We remark again that the flavor condensate analyzed thus far does not require any interaction of the form of Eq. (34), as it stems solely from the misalignment between flavor and mass fields. For neutrino superfluids condensation takes the form

$$\langle \nu^a_L \nu^b_R\rangle = \varepsilon^{ab}D \quad \text{(Dirac)}; \quad \langle \nu_a \bar{\nu}^\dagger_b\rangle = \varepsilon_{ab}D \quad \text{(Majorana)} \tag{35}$$

where, in the first case, condensation occurs between left-handed neutrinos and right-handed neutrinos, and in the second between left-handed neutrinos and right-handed antineutrinos [51]. The symbol ε denotes the Levi-Civita tensor. Notice that for the superfluids considered here, the same number of degrees of freedom is involved for Dirac and Majorana neutrinos, because antineutrinos play no role in the Dirac condensate [50]. The condensates of Eq. (35) can be generalized to many flavors. For definiteness, consider the Dirac case with two flavors, whose general form would read

$$\langle \nu^a_{Lj}\nu^b_{Rk}\rangle = \varepsilon^{ab}D_{jk} \tag{36}$$

with $j, k = 1, 2$. In order to avoid complications in the computation of the capture cross section, we shall actually assume $D_{jk} = \delta_{jk}D_j$, which corresponds to two independent copies, one for each $j = 1, 2$, of the interaction of Eq. (34), without mixed terms. The free Hamiltonian H_0 and the total Hamiltonian H, comprising the interaction terms, can be written as

$$\begin{aligned} H_0 &= \sum_{j=1,2} \int d^3p\, \omega_{\boldsymbol{p};j} \left(a^{(+)\dagger}_{\boldsymbol{p};j} a^{(+)}_{\boldsymbol{p};j} + a^{(-)\dagger}_{\boldsymbol{p};j} a^{(-)}_{\boldsymbol{p};j} \right) \\ H &= \sum_{j=1,2} \int d^3p\, E_{\boldsymbol{p};j} \left(c^{(+)\dagger}_{\boldsymbol{p};j} c^{(+)}_{\boldsymbol{p};j} + c^{(-)\dagger}_{\boldsymbol{p};j} c^{(-)}_{\boldsymbol{p};j} \right) , \end{aligned} \tag{37}$$

where $E_{\boldsymbol{p};j} = \sqrt{(\omega_{\boldsymbol{p};j} - \mu)^2 + \left(\frac{K_j m_{\nu;j}}{\omega_{\boldsymbol{p};j}}\right)^2}$, μ is the chemical potential and $K_j = \frac{h^2_{\nu_j} |D_j|}{2m^2_\sigma}$. The operators c, which diagonalize the full Hamiltonian, are given in terms of the free operators by means of the Bogoliubov transformations

$$\begin{aligned} c^{(+)}_{\boldsymbol{p};j} &= \cos\left(\gamma_j(\boldsymbol{p})\right) e^{-i(\alpha_j + \omega_{\boldsymbol{p};j} t)} a^{(+)}_{\boldsymbol{p};j} - \sin\left(\gamma_j(\boldsymbol{p})\right) e^{i(\alpha_j + \omega_{\boldsymbol{p};j} t)} a^{(-)\dagger}_{-\boldsymbol{p};j} \\ c^{(-)}_{\boldsymbol{p};j} &= \cos\left(\gamma_j(\boldsymbol{p})\right) e^{-i(\alpha_j + \omega_{\boldsymbol{p};j} t)} a^{(-)}_{\boldsymbol{p};j} + \sin\left(\gamma_j(\boldsymbol{p})\right) e^{i(\alpha_j + \omega_{\boldsymbol{p};j} t)} a^{(+)\dagger}_{-\boldsymbol{p};j} , \end{aligned} \tag{38}$$

with $D_j = |D_j| e^{2i\alpha_j}$ and $\tan\left(2\gamma_j(\boldsymbol{p})\right) = \frac{K_j m_{\nu;j}}{\omega_{\boldsymbol{p};j}(\omega_{\boldsymbol{p};j} - \mu)}$. Notice that the antiparticles b play no role in the condensate dynamics. Formally the same Hamiltonians of (37) and the same transformations (38) are valid also in the Majorana case [51]. The quasiparticle operators c define the superfluid vacuum $|0_{SF}\rangle$, satisfying $c^{(s)}_{\boldsymbol{p};j} |0_{SF}\rangle = 0\ \forall s, \boldsymbol{p}, j$. We now come to the computation of the matrix element

$$\langle 0_{SF}| \, \nu_e(x) \, |\nu_{e;\boldsymbol{p},s}\rangle \tag{39}$$

which of course is the only element affected by the condensate in the capture amplitude. The overall effect of the condensate is to change the vacuum state from $|0_M\rangle$ to $|0_{SF}\rangle$. On the other hand the neutrinos involved in the capture process are the free neutrinos, as described by the Hamiltonian H_0. Then the one particle state here refers to

$$|\nu_{e;\boldsymbol{p},j}\rangle = a^{(+)\dagger}_{\boldsymbol{p};e} |0_{SF}\rangle = \left(\cos\Theta a^{(+)\dagger}_{\boldsymbol{p};1} + \sin\Theta a^{(+)\dagger}_{\boldsymbol{p};2}\right) |0_{SF}\rangle \tag{40}$$

that is, to the excitation of a "free" electron neutrino out of the superfluid vacuum. Accordingly $\nu_e(x)$ is the free neutrino field. It is now a simple step, inverting Eqs. (38) and using the canonical anticommutation relations, along with the definition of $|0_{SF}\rangle$, to find the matrix element as

$$\langle 0_{SF}| \, \nu_e(x) \, |\nu_{e;\boldsymbol{p},s}\rangle = \cos^2\Theta \cos^2\left(\gamma_1(\boldsymbol{p})\right) \frac{u^{(s)}_{\boldsymbol{p};1}}{\sqrt{(2\pi)^3}} e^{-i(\omega_{\boldsymbol{p};1} t - \boldsymbol{p}\cdot\boldsymbol{x})} + \sin^2\Theta \cos^2\left(\gamma_2(\boldsymbol{p})\right) \frac{u^{(s)}_{\boldsymbol{p};2}}{\sqrt{(2\pi)^3}} e^{-i(\omega_{\boldsymbol{p};2} t - \boldsymbol{p}\cdot\boldsymbol{x})} . \tag{41}$$

The computation of the capture cross section is now straightforward. Following the same steps described above, we arrive at

$$\sigma_{SF} = \frac{G_F^2}{2\pi} |V_{ud}|^2 F(Z, E) \frac{m_p E_e p_e}{m_n} (f^2 + 3g^2) \left[\cos^4\Theta \cos^4\left(\gamma_1(\boldsymbol{p})\right) + \sin^4\Theta \cos^4\left(\gamma_2(\boldsymbol{p})\right)\right] . \tag{42}$$

Remarkably, this expression shows an additional $\boldsymbol{p}$ dependency with respect to the Pontecorvo case (24), a feature it shares with σ_{PD} and σ_F of eqs. (26) and (27). Similarly, in addition to the extra $\boldsymbol{p}$ dependency, the net effect of the condensate is to lower the Pontecorvo value, due to the $\cos\gamma$ factors. This is consistent with our previous findings about the flavor condensate of the flavor Fock space approach. Because the treatment is formally equivalent for Majorana neutrinos, the result is identical, except for a factor of two arising in the capture rate [34], which is common to all the frameworks considered here.

5. Conclusions

We have analyzed the possibility to test the QFT of neutrino mixing and the predicted contribution of the flavor vacuum to the dark matter by means of low energy neutrino capture experiments. We have considered the possible schemes of neutrino mixing and the related flavor states definition in the computation of the capture rate of neutrino absorption by tritium. We have shown that the capture cross section and the capture rate depend on the definition of the flavor states and are significantly different for very small neutrino momenta $p_\nu \simeq m_\nu$. This amounts to an observable trace of the Bogoliubov coefficients that characterize the condensation of the flavor vacuum in the flavor Fock space model. Therefore, experiments such as PTOLEMY, projected to reveal the cosmic neutrino background (neutrinos with momenta $p_\nu \simeq m_\nu$), can not only distinguish among the possible mixing schemes, but also provide an indirect evidence of the flavor condensate and of the dark matter contribution induced by the neutrino mixing. An analogous mechanism of flavor condensation is also predicted for mixed bosons [45] and the possible role of the boson flavor vacuum as a dark energy component has been investigated [29]. Future studies on the pure annihilation type radiative B meson decays $B^0 \to \phi\gamma$ and $B_s \to \rho^0(\omega)\gamma$ [46] and on $\omega - \phi$ meson mixing [47], could allow the detection of observable signatures of the boson flavor vacuum condensation in meson mixing phenomena. Due to the larger mass differences involved with respect to neutrino mixing, it is reasonable to prospect even more significant observable effects on meson mixing, due to the structure of the flavor vacuum.

Declaration of competing interest

The authors declare that they have no known competing financial interests or personal relationships that could have appeared to influence the work reported in this paper.

Data availability

No data was used for the research described in the article.

Acknowledgements

Partial financial support from MIUR and INFN is acknowledged. A.C. also acknowledges the COST Action CA1511 Cosmology and Astrophysics Network for Theoretical Advances and Training Actions (CANTATA).

Appendix A. Cross section for generalized amplitude

In this appendix we work out the cross section for amplitudes containing more than one energy delta function. Following Weinberg [48] the differential probability for the $I \to F$ transition is

$$dP(I \to F) = \left[\frac{(2\pi)^3}{V}\right]^{N_I} |S_{FI}|^2 dF \tag{A.1}$$

where N_I is the number of particles in the state $|I\rangle$, dF is the phase space volume element for the final state and we are assuming that the system is confined in a box of volume V. Likewise, we assume that the interaction is switched on for a finite time T. Suppose that the S- matrix has the form

$$S_{FI} = -2\pi i \delta_V^3(\boldsymbol{P}_F - \boldsymbol{P}_i) \sum_j \delta_T(E_{I,j} - E_F) M_{FI;j} \,. \tag{A.2}$$

Here $\delta_V^3(\boldsymbol{p}) = \frac{1}{(2\pi)^3}\int_V d^3x e^{i\boldsymbol{p}\cdot\boldsymbol{x}}$ and $\delta_T(E) = \frac{1}{2\pi}\int_{-\frac{T}{2}}^{\frac{T}{2}} dt e^{-iEt}$ are the finite volume and the finite time delta functions. The matrix elements $M_{FI;j}$ refer to the processes in which the initial state has total energy $E_{I,j}$, total momentum $\boldsymbol{P}_I$ and the final state has total energy E_F and total momentum $\boldsymbol{P}_F$. Upon squaring the S-matrix element of eq. (A.2) we shall get mixed terms proportional to distinct delta functions $\propto \delta_T(E_{I,j} - E_F)\delta_T(E_{I,j'} - E_F)$. These terms impose incompatible conditions on the final energy ($E_F = E_{I,j} = E_{I,j'}$, whereas $E_{I,j} \neq E_{I,j'}$ by hypothesis) and therefore yield a zero contribution. The only surviving terms are those with the same energy delta function:

$$|S_{FI}|^2 = (2\pi)^2 \left[\delta_V^3(\boldsymbol{P}_F - \boldsymbol{P}_i)\right]^2 \sum_j \left[\delta_T(E_{I,j} - E_F)\right]^2 |M_{FI;j}|^2 \,. \tag{A.3}$$

The squared delta functions can be easily interpreted within the finite volume and finite time hypothesis [48], giving for the differential probability

$$dP(I \to F) = (2\pi)^2 \left[\frac{(2\pi)^3}{V}\right]^{N_I - 1} \frac{T}{2\pi} \delta_V^3(\boldsymbol{P}_F - \boldsymbol{P}_i) \sum_j \delta_T(E_{I,j} - E_F)|M_{FI;j}|^2 \,. \tag{A.4}$$

Specializing to $N_I = 2$ and taking the infinite volume/infinite time limits the differential cross section is

$$d\sigma(I \to F) = \frac{dP(I \to F)}{u_I}\frac{V}{T} = (2\pi)^4 u_I^{-1} \sum_j \delta^4(P^\mu_{I;j} - P^\mu_F)|M_{FI;j}|^2 dF \tag{A.5}$$

where u_I is the relative velocity.

Appendix B. Flavor ladder operators

The Pontecorvo mixing relations for two flavors are [9,10]

$$\begin{aligned} \nu_e(x) &= \nu_1(x)\cos\Theta + \nu_2(x)\sin\Theta \\ \nu_\mu(x) &= -\nu_1(x)\sin\Theta + \nu_2(x)\cos\Theta \end{aligned} \tag{B.1}$$

where $\nu_e(x)$ and $\nu_\mu(x)$ are the Dirac neutrino fields with definite flavors. $\nu_1(x)$ and $\nu_2(x)$ are the free neutrino fields with definite masses m_1 and m_2, respectively. The fields $\nu_1(x)$ and $\nu_2(x)$ are written as

$$\nu_i(x) = \int \frac{d^3k}{(2\pi)^{\frac{3}{2}}} \sum_r \left[u^r_{\mathbf{k},i}\, a^r_{\mathbf{k},i}(t) + v^r_{-\mathbf{k},i}\, b^{r\dagger}_{-\mathbf{k},i}(t)\right] e^{i\mathbf{k}\cdot\mathbf{x}}, \qquad i = 1,2, \tag{B.2}$$

with

$$u^1_{\mathbf{k},i} = \left(\frac{\omega_{k,i} + m_i}{2\omega_{k,i}}\right)^{\frac{1}{2}} \begin{pmatrix} 1 \\ 0 \\ \frac{k_3}{\omega_{k,i}+m_i} \\ \frac{k_1+ik_2}{\omega_{k,i}+m_i} \end{pmatrix}; \qquad u^2_{\mathbf{k},i} = \left(\frac{\omega_{k,i} + m_i}{2\omega_{k,i}}\right)^{\frac{1}{2}} \begin{pmatrix} 0 \\ 1 \\ \frac{k_1-ik_2}{\omega_{k,i}+m_i} \\ \frac{-k_3}{\omega_{k,i}+m_i} \end{pmatrix}; \tag{B.3}$$

$$v^1_{-\mathbf{k},i} = \left(\frac{\omega_{k,i} + m_i}{2\omega_{k,i}}\right)^{\frac{1}{2}} \begin{pmatrix} \frac{-k_3}{\omega_{k,i}+m_i} \\ \frac{-k_1-ik_2}{\omega_{k,i}+m_i} \\ 1 \\ 0 \end{pmatrix}; \qquad v^2_{-\mathbf{k},i} = \left(\frac{\omega_{k,i} + m_i}{2\omega_{k,i}}\right)^{\frac{1}{2}} \begin{pmatrix} \frac{-k_1+ik_2}{\omega_{k,i}+m_i} \\ \frac{k_3}{\omega_{k,i}+m_i} \\ 0 \\ 1 \end{pmatrix}; \tag{B.4}$$

$a^r_{\mathbf{k},i}(t) = a^r_{\mathbf{k},i}\, e^{-i\omega_{k,i}t}$, $b^{r\dagger}_{\mathbf{k},i}(t) = b^{r\dagger}_{\mathbf{k},i}\, e^{i\omega_{k,i}t}$, and $\omega_{k,i} = \sqrt{\mathbf{k}^2 + m_i^2}$. The operator $a^r_{\mathbf{k},i}$ and $b^r_{\mathbf{k},i}$, $i = 1, 2$, $r = 1, 2$, are the annihilation operators for the vacuum state $|0\rangle_{1,2} \equiv |0\rangle_1 \otimes |0\rangle_2$: $a^r_{\mathbf{k},i}|0\rangle_{12} = b^r_{\mathbf{k},i}|0\rangle_{12} = 0$.

The Eqs. (B.1) relate the respective Lagrangians $\mathcal{L}_{1,2}$ and $\mathcal{L}_{e,\mu}$ [9,10]:

$$\mathcal{L}_{1,2} = i\bar{\nu}_1\gamma^\rho\partial_\rho\nu_1 + i\bar{\nu}_2\gamma^\rho\partial_\rho\nu_2 - (m_1\,\bar{\nu}_1\nu_1 + m_2\,\bar{\nu}_2\nu_2) \tag{B.5}$$

$$\mathcal{L}_{e,\mu} = i\bar{\nu}_e\gamma^\rho\partial_\rho\nu_e + i\bar{\nu}_\mu\gamma^\rho\partial_\rho\nu_\mu - \big(m_{ee}\,\bar{\nu}_e\nu_e + m_{\mu\mu}\,\bar{\nu}_\mu\nu_\mu + m_{e\mu}\left(\bar{\nu}_e\nu_\mu + \bar{\nu}_\mu\nu_e\right)\big) \tag{B.6}$$

where

$$m_{ee} = m_1\cos^2\Theta + m_2\sin^2\Theta, \tag{B.7}$$

$$m_{\mu\mu} = m_1\sin^2\Theta + m_2\cos^2\Theta, \tag{B.8}$$

$$m_{e\mu} = (m_2 - m_1)\sin\Theta\cos\Theta. \tag{B.9}$$

The Lagrangian and the field equations, in QFT, are expressed by means of the interacting (or Heisenberg) fields. On the other hand the observables are given in terms of asymptotic (free) fields. The asymptotic fields are given by the weak limit (at $t \to \pm\infty$) of the interacting fields. The weak limit implies that the realization of the dynamics in terms of the asymptotic fields is not unique, but is representation-dependent. Such dependency is due to the existence of infinitely many unitarily inequivalent representations of the canonical anticommutation relations in QFT [26,49].[4] Given that the observables are expressed in terms of the asymptotic fields, unitarily inequivalent representations describe inequivalent physical phases. It is therefore important to use care in the study of the mapping between the free and interacting fields, also known as the dynamical map or Haag expansion [26,49], in order to get meaningful results. As discussed above, this point pertains the systems with an infinite number of degrees of freedom, as in QFT, for which the Stone-Von Neumann theorem does not hold. These aspects also characterize the field mixing, where two specific Fock spaces arise: $\mathcal{H}_{12}$ for the free fields ν_1, ν_2 and $\mathcal{H}_{e\mu}$ for the interacting fields ν_e, ν_μ. In the infinite volume limit $\mathcal{H}_{12}$ and $\mathcal{H}_{e\mu}$ turn out to be mutually orthogonal. Introducing the generator $G_\Theta(t)$ the mixing transformations (B.1) read [23]:

$$\nu_e(x) = G^{-1}_{\mathbf{\Theta}}(t)\;\nu_1(x)\;G_{\mathbf{\Theta}}(t) \tag{B.10}$$
$$\nu_\mu(x) = G^{-1}_{\mathbf{\Theta}}(t)\;\nu_2(x)\;G_{\mathbf{\Theta}}(t)$$

where $G_{\mathbf{\Theta}}(t)$ is given by

$$G_{\mathbf{\Theta}}(t) = exp\left[\Theta\int d^3\mathbf{x}\left(\nu_1^\dagger(x)\nu_2(x) - \nu_2^\dagger(x)\nu_1(x)\right)\right] = exp\left\{\Theta\int d^3\mathbf{x}\,[(\nu_1,\nu_2)_t - (\nu_2,\nu_1)_t]\right\}. \tag{B.11}$$

$G_{\mathbf{\Theta}}(t)$, at finite volume is a unitary operator: $G^{-1}_{\mathbf{\Theta}}(t) = G_{-\mathbf{\Theta}}(t) = G^\dagger_{\mathbf{\Theta}}(t)$, preserving the canonical anticommutation relations. Notice that Eq. ((B.11)) is derived by taking into account the relations

$$d^2\nu_e/d\Theta^2 = -\nu_e\;,\quad d^2\nu_\mu/d\Theta^2 = -\nu_\mu\;, \tag{B.12}$$

and the boundary conditions

$$\nu_e|_{\Theta=0} = \nu_1,\quad d\nu_e/d\Theta|_{\Theta=0} = \nu_2 \quad\text{and}\quad \nu_\mu|_{\Theta=0} = \nu_2,\quad d\nu_\mu/d\Theta|_{\Theta=0} = -\nu_1\;. \tag{B.13}$$

We can see that the operator $G_{\mathbf{\Theta}}(t)$ generates Eqs. (B.1).

We now determine the relation between the Hilbert spaces for free fields $\mathcal{H}_{1,2}$ and interacting fields $\mathcal{H}_{e,\mu}$ by considering the generic matrix element ${}_{1,2}\langle a|\nu_1(x)|b\rangle_{1,2}$ (a similar argument holds for $\nu_2(x)$), where $|a\rangle_{1,2}$ is the generic element of $\mathcal{H}_{1,2}$. Inverting the first of Eqs. (B.10), we deduce:

$${}_{1,2}\langle a|G_{\mathbf{\Theta}}(t)\;\nu_e(x)\;G^{-1}_{\mathbf{\Theta}}(t)|b\rangle_{1,2} \;=\; {}_{1,2}\langle a|\nu_1(x)|b\rangle_{1,2}\;. \tag{B.14}$$

The field ν_e is defined on $\mathcal{H}_{e,\mu}$, then the vector $G^{-1}_{\mathbf{\Theta}}(t)|a\rangle_{1,2}$ belongs to $\mathcal{H}_{e,\mu}$, and thus $G^{-1}_{\mathbf{\Theta}}(t)$ maps $\mathcal{H}_{1,2}$ to $\mathcal{H}_{e,\mu}$, that is $G^{-1}_{\mathbf{\Theta}}(t) : \mathcal{H}_{1,2} \mapsto \mathcal{H}_{e,\mu}$. The flavor vacuum, that is the vacuum for the flavor Hilbert space $\mathcal{H}_{e,\mu}$, is given by

$$|0(t)\rangle_{e,\mu} = G^{-1}_{\mathbf{\Theta}}(t)\;|0\rangle_{1,2}\;. \tag{B.15}$$

Since $G_{\mathbf{\Theta}}(t)$ is linear, the annihilators for the flavor vacuum (or flavor ladder operators), relative to the fields $\nu_e(x)$ and $\nu_\mu(x)$ at each time satisfy

$$a^r_{\mathbf{k},\nu_e}(t)\;|0(t)\rangle_{e,\mu} = G^{-1}_{\mathbf{\Theta}}(t)\;a^r_{\mathbf{k},1}(t)\;|0\rangle_{1,2} = 0,$$

[4] In the case of neutrinos, the Heisenberg dynamics of the fields is independent on the choice of the basis (mass or flavor basis). Indeed the solution of the Heisenberg equations can be equivalently put in terms of flavor fields and mass fields. On the other hand the asymptotic realization of such dynamics is not unique, and the physical observables depend on the choice of the asymptotic fields. In particular, when considering weak interaction processes, in which neutrinos are produced, the particle content of the theory, and the corresponding observables, depend on whether the asymptotic neutrino fields are mass fields or flavor (oscillating) fields. In this case, since neutrinos are produced and detected as flavor neutrinos, the natural choice for the representation corresponds to asymptotic flavor fields. This situation is reminiscent of the processes where particle creation occurs, such as the Hawking-Unruh effect, the Casimir effect, the Parker effect or the Schwinger effect. For these phenomena the Heisenberg dynamics is the same as the free dynamics, but different boundary conditions lead to distinct particle interpretations of the theory.

and are then given by

$$a^r_{\mathbf{k},\nu_e}(t) \equiv G^{-1}_{\boldsymbol{\Theta}}(t)\, a^r_{\mathbf{k},1}(t)\, G_{\boldsymbol{\Theta}}(t)\,, \tag{B.16}$$

and similar for ν_μ and the antiparticles.

The flavor operators are computed explicitly as

$$a^r_{\mathbf{k},\nu_e}(t) = \cos\Theta\, a^r_{\mathbf{k},1}(t) \,+\, \sin\Theta \sum_s \left[u^{r\dagger}_{\mathbf{k},1}\, u^s_{\mathbf{k},2}\, a^s_{\mathbf{k},2}(t) \,+\, u^{r\dagger}_{\mathbf{k},1}\, v^s_{-\mathbf{k},2}\, b^{s\dagger}_{-\mathbf{k},2}(t) \right]\,, \tag{B.17}$$

and similar for $a_{\nu_\mu}, b_{\nu_e}, b_{\nu_\mu}$. When $\boldsymbol{k}$ is directed along the third axis $\boldsymbol{k} = (0, 0, |\boldsymbol{k}|)$, the helicities decouple and one has the simpler form:

$$a^r_{\mathbf{k},\nu_e}(t) = \cos\Theta\, a^r_{\mathbf{k},1}(t) \,+\, \sin\Theta\, \left(|U_{\mathbf{k}}|\, a^r_{\mathbf{k},2}(t) \,+\, \epsilon^r\, |V_{\mathbf{k}}|\, b^{r\dagger}_{-\mathbf{k},2}(t) \right) \tag{B.18}$$

with $\epsilon^r = (-1)^r$ and

$$|U_{\mathbf{k}}| \equiv u^{r\dagger}_{\mathbf{k},i} u^r_{\mathbf{k},j} = v^{r\dagger}_{-\mathbf{k},i} v^r_{-\mathbf{k},j}\,, \qquad |V_{\mathbf{k}}| \equiv \epsilon^r\, u^{r\dagger}_{\mathbf{k},1} v^r_{-\mathbf{k},2} = -\epsilon^r\, u^{r\dagger}_{\mathbf{k},2} v^r_{-\mathbf{k},1}$$

where $i, j = 1, 2$ and $i \neq j$. We remark that the mass $|0_M\rangle$ and the flavor vacuum $|0_F(t)\rangle$ are orthogonal to each other for any t, in the infinite volume limit. The same is also true for the flavor vacua at different times, that is $\lim_{V\to\infty} \langle 0_F(t')|\, 0_F(t)\rangle = 0$ for $t \neq t'$.

References

[1] Super-Kamiokande Collaboration, Y. Fukuda, et al., Phys. Rev. Lett. 81 (1998) 1562.
[2] Double Chooz Collaboration, Y. Abe, et al., Phys. Rev. Lett. 108 (2012) 131801.
[3] F.P. An, et al., Phys. Rev. Lett. 108 (2012) 171803.
[4] T2K Collaboration, K. Abe, et al., Phys. Rev. D 88 (2013) 032002.
[5] H. Georgi, S.L. Glashow, Phys. Rev. Lett. 32 (1974) 438–441;
J. Wess, B. Zumino, Nucl. Phys. B 70 (1974) 39–50.
[6] A. Capolupo, S.M. Giampaolo, A. Quaranta, Phys. Lett. B 820 (2021) 136489.
[7] J. Ellis, Nucl. Phys. A 827 (2009) 1;
P. Salucci, et al., Front. Phys. 8 (2021).
[8] F. Wilczek, Phys. Rev. Lett. 40 (1978) 279–282;
R.D. Peccei, H.R. Quinn, Phys. Rev. Lett. 38 (1977) 1440–1443;
G. Raffelt, L. Stodolsky, Phys. Rev. D 37 (1988) 1237–1249;
A. Capolupo, G. Lambiase, A. Quaranta, S.M. Giampaolo, Phys. Lett. B 804 (2020) 135407;
A. Capolupo, S.M. Giampaolo, A. Quaranta, Eur. Phys. J. C 81 (2021) 1116.
[9] S.M. Bilenky, B. Pontecorvo, Phys. Rep. 41 (4) (1978) 225–261.
[10] S.M. Bilenky, S.T. Petcov, Rev. Mod. Phys. 59 (1987) 671–754.
[11] W. Buchmüller, R.D. Peccei, T. Yanagida, Annu. Rev. Nucl. Part. Sci. 55 (2005) 311–355.
[12] A. Abada, G. Arcadi, V. Domcke, M. Lucente, J. Cosmol. Astropart. Phys. 12 (2017) 024.
[13] V.C. Rubin, W.K. Ford Jr., Astron. J. 159 (1970).
[14] V. Trimble, Annu. Rev. Astron. Astrophys. 25 (1) (1987) 425–472.
[15] L. Perivolaropoulos, F. Skara, Challenges for ΛCDM: an update, arXiv:2105.05208v3, 2022.
[16] S. Clesse, J. García-Bellido, Phys. Dark Universe 22 (2018) 137–146.
[17] P.H. Frampton, M. Kawasaki, F. Takahashi, T.T. Yanagida, J. Cosmol. Astropart. Phys. 04 (2010) 023.
[18] G. Jungman, M. Kamionkowski, K. Griest, Phys. Rep. 267 (5–6) (1996) 195–373.
[19] M. Kawasaki, K. Nakayama, Annu. Rev. Nucl. Part. Sci. 63 (2013) 69–95.
[20] L.D. Duffy, K. van Bibber, New J. Phys. 11 (2009) 105008.
[21] F. Chadha-Day, J. Ellis, D.J.E. Marsh, Sci. Adv. 8 (2022) 8.
[22] A. Boyarsky, M. Drewes, T. Lasserre, S. Mertens, O. Ruchayskiy, Prog. Nucl. Part. Phys. 104 (2019) 1–45.
[23] E. Alfinito, M. Blasone, A. Iorio, G. Vitiello, Phys. Lett. B 362 (1995) 91;
M. Blasone, A. Capolupo, G. Vitiello, Phys. Rev. D 66 (2002) 025033, and reference therein;
M. Blasone, A. Capolupo, S. Capozziello, S. Carloni, G. Vitiello, Phys. Lett. A 323 (2004) 182–189.
[24] C.-R. Ji, Y. Mishchenko, Phys. Rev. D 65 (2002) 096015.
[25] A. Capolupo, C.-R. Ji, Y. Mishchenko, G. Vitiello, Phys. Lett. B 594 (1–2) (2004) 135–140;
A. Capolupo, A. Quaranta, P. Setaro, Phys. Rev. D 106 (2022) 043013.
[26] H. Umezawa, H. Matsumoto, M. Tachiki, Thermo Field Dynamics and Condensed States, North Holland, 1982;
H. Umezawa, Advanced Field Theory: Micro, Macro and Thermal Physics, American Institute of Physics, New York, 1993;
N.N. Bogoliubov, A.A. Logunov, A.I. Oksak, I.T. Todorov, General Principles of Quantum Field Theory, Kluwer Academic Publishers, 1990.
[27] K.C. Hannabuss, D.C. Latimer, J. Phys. A 33 (2000) 1369.
[28] A. Capolupo, S. Carloni, A. Quaranta, Phys. Rev. D 105 (2022) 105013.
[29] A. Capolupo, Adv. High Energy Phys. 2016 (2016) 8089142.
[30] A. Capolupo, Adv. High Energy Phys. 2018 (2018) 9840351.
[31] A. Capolupo, S. Capozziello, G. Vitiello, Phys. Lett. A 373 (6) (2009) 601–610.
[32] A. Capolupo, S. Capozziello, G. Vitiello, Phys. Lett. A 363 (1) (2007) 53–56.
[33] PTOLEMY Collaboration, M.G. Betti, et al., J. Cosmol. Astropart. Phys. 07 (2019) 047.
[34] A.J. Long, C. Lunardini, E. Sabancilar, J. Cosmol. Astropart. Phys. 08 (2014) 038.
[35] A. Faessler, R. Hodak, S. Kovalenko, F. Šimkovic, Int. J. Mod. Phys. E 26 (01n02) (2017) 1740008;
arXiv:1602.03347v1, 2016.
[36] A. Capolupo, G. Lambiase, A. Quaranta, Phys. Rev. D 101 (2020) 095022.
[37] A. Capolupo, S.M. Giampaolo, G. Lambiase, A. Quaranta, Eur. Phys. J. C 80 (2020) 423.
[38] C.-Y. Lee, Mod. Phys. Lett. A 35 (29) (2020).
[39] J. Alvey, M. Escudero, N. Sabti, T. Schwetz, Phys. Rev. D 105 (2021) 063501.
[40] J.L. Bernal, A. Caputo, F. Villaescusa-Navarro, M. Kamionkowski, Phys. Rev. Lett. 127 (2021) 131102.
[41] P.A. Zyla, et al., Particle Data Group, Prog. Theor. Exp. Phys. 2020 (2020) 083C01, and 2021 update.

[42] A. Capolupo, S.M. Giampaolo, G. Lambiase, Phys. Lett. B 792 (2019) 298–303;
L. Buoninfante, A. Capolupo, S.M. Giampaolo, G. Lambiase, Eur. Phys. J. C 80 (2020) 1009;
A. Capolupo, S.M. Giampaolo, G. Lambiase, A. Quaranta, Universe 6 (11) (2020) 207.
[43] M. Blasone, A. Capolupo, C.-R. Ji, G. Vitiello, Int. J. Mod. Phys. A 25 (22) (2010) 4179–4194.
[44] K. Akita, S. Hurwitz, M. Yamaguchi, Eur. Phys. J. C 81 (2021) 344.
[45] M. Blasone, A. Capolupo, O. Romei, G. Vitiello, Phys. Rev. D 63 (2001) 125015.
[46] H. Deng, et al., Phys. Rev. D 103 (2021) 076004.
[47] A. Kucukarslan, Ulf-G. Meißner, Mod. Phys. Lett. A 21 (18) (2006) 1423–1430.
[48] S. Weinberg, The Quantum Theory of Fields, vol. I: Foundations, first edition, Cambridge University Press, 1995.
[49] C. Itzykson, J.B. Zuber, Quantum Field Theory, McGraw-Hill, New York, 1980;
S. Schweber, An Introduction to Relativistic Quantum Field Theory, Harper and Row, 1961.
[50] J.I. Kapusta, Phys. Rev. Lett. 93 (2004) 251801.
[51] J.R. Bhatt, U. Sarkar, Phys. Rev. D 80 (2009) 045016.